Holographic Descriptions of Magnetic Effect on Chiral Field Theory

by

Namshik Kim

M.Sc., Yonsei University, 2009

A THESIS SUBMITTED IN PARTIAL FULFILLMENT OF
THE REQUIREMENTS FOR THE DEGREE OF

MASTER OF SCIENCE

in

The Faculty of Graduate Studies

(Physics)

THE UNIVERSITY OF BRITISH COLUMBIA

(Vancouver)

October, 2011

Abstract

In this thesis, we will study a top-down string theory holographic model of strongly interacting relativistic 2+1 dimensional fermions. We study the defect theory as examining a charged probe D7-branes/anti-branes model and a charged probe D5-branes/anti-branes model on the thermal $AdS_5 \times S^5$ geometry. We use the branes pair model to depict a geometrical chiral symmetry breaking. We are especially interested in the holographic magnetic effect on the flavour symmetries.

Table of Contents

List of Tables

List of Figures

Acknowledgements

I would like to thank Gordon Semenoff. He was always generous and the wisest supervisor. I learned a lot from him how to treat the problems in physics. He showed me his big patience and made my point of view widen in the theoretical physics.

Thank my parents and my sister for their incredible supports and trust.

I would also like to thank Josh who was my colleague as well as helper for my recent researches.

To My Parents.

Chapter 1

Introduction

To illuminate the phenomena of strongly interacting systems has been an important task of physicists. Perturbative methods which were strong arms of physicists to apprehend weakly coupled systems do not work any more in these research fields.

Gravity/gauge theory duality(or *AdS/CFT correspondence*) was first suggested by Maldacena [1], and it has been researched by many theorists since it is one of the most powerful candidates to figure out the strongly interacting system. The essence of this argument is that it makes it possible to use a weakly coupled supergravity theory to research a strongly coupled large N gauge theory. Though it is of use only for large N gauge case, to survey the AdS/CFT correspondence provides lots of deep intuitions and knowledges for particle physics and condensed matter physics. There are a great deal of unsolved problems in a 2+1 dimensional field theory related to strongly coupled systems. It is worth researching graphene [2], topological insulators, high temperature superconductors, quantum phase transition [3] and so on by using this special duality.

The most famous example of this duality argued by Maldacena is the duality between Type IIB string theory on $AdS_5 \times S^5$ spacetime and $\mathcal{N} = 4$[I] supersymmetric YangMills gauge theory which is a conformal field theory on the 4-dimensional boundary of 4 dimensional spacetime, AdS_5. It is why it is called *a holographic theory*.

[I] Here $\mathcal{N}$ is the number of SUSY operators.

It was researched how to add flavours to AdS/CFT by [4]. Using the idea, we consider a number of stacks Dp-branes, $N_c \to \infty$, constructing the supergravity background geometry. Then introduce several stacks of probe Dq-branes, and consider a quenched approximation as a probe limit, $N_f \ll N_c$ where N_f is the number of the probed Dq-branes giving flavours. Now we can ignore the back-reaction on the supergravity background geometry, and can study a dynamics considering probed D-branes by simply using the DBI action and WZ term. Dq-branes can be probed on the $AdS_5 \times S^5$ geometry to construct a defect field theory. The probed branes extend along 2+1 dimensional subspace of the 4 dimensional boundary of the $AdS_5 \times S^5$ spacetime. The full dual field theory lives at the asymptotic 3+1 dimensional boundary of this 9+1 dimensional spacetime and the defect theory lives where the probe brane intersects the boundary. We will introduce probed D5-, D7-branes on the $AdS_5 \times S^5$ to support the defect field theory in the thesis.

Sakai and Sugimoto could consider a chiral fermionic gauge theory as embedding $D8/\bar{D}8$ branes on the compactified 5th coordinate of D4-branes with the probe limit, $N_8 \ll N_4$. The compacitified 5th coordinate has an anti-periodic boundary condition for the fermions on the D4-branes in order to break supersymmetry and to make unwanted fields become massive and integrating out. They used the cigar-like geometrical model in the near horizon geometry of the sugra solution. Then the compactification is emergent, and this geometry necessarily leads to a joined solution meaning spontaneously broken chiral symmetry. It has a 4 dimensional boundary and gives a chiral model to survey QCD. The D4/D8 open strings have ♯ND=6. Supersymmetry is broken, and the NS sector is massive, but the R sector is still massless. [5] [6] [17]

On the other hand, as assuming the supergravity background with the high temperature, we should compactify the Euclidean time coordinate instead of the 5th coordinate.[5] The geometry loses the cigar-like embedding.

Since the geometry does not require the joined solution any more, we should be careful to see whether the symmetry is breaking or not. This property of the branes/anti-branes pair is very related to confinement/deconfinement in field theory. Besides, when the temperature increases, geometrically the size of the black holes becomes bigger, and the branes/anti-branes pair can attach to the black holes horizon. Thus, black holes cease the connection between branes and anti-branes. In other words, the chiral symmetry is thermally restored.[7]

If we take a decompacified limit of the Sakai-Sugimoto model, it is known that the supergravity background yields a stringy NJL model as suggested by [15]. The configuration for the chiral symmetry breaking becomes clearer since confinement/deconfinement is not concerned any more in this geometry. The separation of the boundary is dual to effective coupling of 4 fermions interaction.

It has been known that the presence of an external magnetic field enhances the tendency of gauge theory interactions to break chiral symmetry and to generate a fermion dynamic mass in 2+1 dimensions. This phenomenon has been called *magnetic catalysis*.[10] [11] [II] It would be very interesting to understand this phenomenon at the strong interacting systems. This question has been addressed and answered in the recent series of papers where AdS/CFT duality is used to construct a holographic dual of a 2+1-dimensional field theory with chiral symmetry. Chiral symmetry breaking is found in the presence of an external magnetic field in various environments given by temperature, other fluxes and densities.

In the present paper, we will study a top-down string theory holographic model of strongly interacting relativistic 2+1 dimensional fermions. We

[II] To speak more exactly, in a 2+1 dimension, we cannot argue a chiral symmetry by the fact that fermions are not chiral in odd dimensions.[17]. It is a dynamical flavour symmetry rather than a chiral one. Nevertheless, I might use the word "chiral symmetry" frequently in this thesis. Some physicists use it conventionally.

will study and compare various branes/anti-branes pair embeddings on the thermal $AdS_5 \times S^5$ geometry. We are especially interested in the holographic magnetic effect in the branes/anti-branes pair solutions.

The remainder of the paper will be organized as follows. In chapter 2, we will construct the D3/D7-branes model concretely. We will write down the full action of this model including DBI and WZ actions, too. In chapter 3, we will obtain the Routhians using the action we acquire in the previous chapter 2, and investigate the BF bound of the scalar field as a fluctuation along the coordinate of D7-branes. It will provide the stable embedding condition for D3/D7-branes model. In chapters 4 and 6 which are our main parts of this paper, we will orderly construct $D7/\bar{D}7$-branes, $D5/\bar{D}5$-branes, $D5/\bar{D}5$-branes model on the thermal D3-branes background, and classify and explain the two possible joined solutions model. We will see the concrete phenomenon from the magnetic field in these chapters by using numerical plots. In chapter 7, we will briefly review how the internal fluxes introduced on probed branes change the rank of the SYM gauge group in the separate regions by probed branes in D3/D5-branes pairs. Besides, we will briefly introduce the domain wall as a 2+1 dimensional defect conformal field theoretical object.

Chapter 2

Construction of D3/D7-branes Model

2.1 $S^2 \times S^2$ Embedding

We can consider a simple brane configuration has only purely charged fermioinic theory in 2+1 dimensions at low energy from constructing D3/D7 branes model. We think the near horizon background geometry of thermal D3-branes, and then consider a D7-branes embedding wraps an $S^2 \times S^2$ by using the idea suggested by [8], [9]. Thus, we begin with following geometric description of the thermal D3-branes.

$$L^{-2}ds^2 = r^2\big(-h(r)dt^2 + dx^2 + dy^2 + dz^2\big) + \frac{dr^2}{h(r)r^2} + d\Omega_5^2 \tag{2.1}$$

where

$$\begin{aligned} h(r) &= 1 - \frac{r_h^4}{r^4} && (2.2)\\ L^4 &= 4\pi g_s N_3 \alpha'^2 && (2.3)\\ d\Omega_5^2 &= d\psi^2 + \sin^2\psi d\Omega_2^2 + \cos^2\psi d\tilde{\Omega}_2^2 && (2.4)\\ F_5 = dC_4 &= \frac{4L^4}{g_s}(r^3 dt \wedge dx \wedge dy \wedge dz \wedge dr + d\Omega_5) && (2.5) \end{aligned}$$

We set Ramond-Ramond form vanishes at the horizon, $r = r_h$. Then C_4 is

$$\frac{g_s}{L^4}C_4 = r^4 h(r) dt \wedge dx \wedge dy \wedge dz + \frac{1}{2}\Big(\psi - \frac{1}{4}\sin(4\psi) + c_0\Big)d\Omega_2 \wedge d\tilde{\Omega}_2. \tag{2.6}$$

because

$$c(\psi) \equiv (8\pi^2 L^4)^{-1} \int_{S^2\times S^2} C_4 = \psi - \frac{1}{4}\sin(4\psi) + c_0 \tag{2.7}$$

Now we probe D7-branes, which wrap an $S^2 \times S^2$ and extend along t, x, y and r. In the near horizon limit, D7 branes are extended along AdS_4, and wrap an S^4. We demand this probe to construct a defect 2+1 dimensional field theory. Now our defect constructions are described by the following array:

	0	1	2	3	4	5	6	7	8	9
$D3$	•	•	•	•	–	–	–	–	–	–
$D7$	•	•	•	–	•	•	•	•	•	–

(2.8)

We consider the following probe *ansatz*, $z = z(r)$ and $\psi = \psi(r)$. To simplify the solution, we will require constant ψ. The asymptotic separation between the D3- and D7-branes corresponds to the mass of the hypermultiplet. In this case, supersymmetries diminish, and the defect theory supports N_f flavours of fermions.[14]

2.2 Probe Branes Action

We also introduce an external magnetic field as well as electric field with fluxes on two S^2. The gauge field profile is

$$\begin{aligned} F &= F_{rt}(r)dr \wedge dt + F_{xy}(r)\, dx \wedge dy \\ &\qquad + F_{\theta\phi}(r)d\theta \wedge d\phi + F_{\tilde{\theta}\tilde{\phi}}(r)d\tilde{\theta} \wedge d\tilde{\phi} \qquad (2.9) \\ &= \frac{L^2}{2\pi\alpha'}\Big(\dot{A}_0(r)dr \wedge dt + B\, dx \wedge dy + \frac{f_1}{2}d\Omega_2 + \frac{f_2}{2}d\tilde{\Omega}_2\Big) \qquad (2.10) \end{aligned}$$

where $\dot{A}_0 \equiv \frac{dA}{dr}$.

The induced metric on the D7-branes is described by

$$L^{-2}ds^2 = r^2\big(-h(r)dt^2 + dx^2 + dy^2\big) + \frac{1 + r^2h\dot{\psi}^2 + r^4h\dot{z}^2}{h(r)r^2}dr^2 + \sin^2\psi d\Omega_2^2 + \cos^2\psi d\tilde{\Omega}_2^2 \quad (2.11)$$

and the DBI action of Minkowski embedding is

$$S_{DBI} = -\mathcal{N}_7 \int_{r_0}^{\infty} dr \sqrt{V(r,\psi)(1 + r^2h\dot{\psi}^2 + r^4h\dot{z}^2 - \dot{A}^2)} \quad (2.12)$$

where

$$V(\psi, r) = (r^4 + B(r)^2)(f_1^2 + 4\sin^4\psi)(f_2^2 + 4\cos^4\psi) \quad (2.13)$$

$$\mathcal{N}_7 = \frac{4\pi^2 N_7 T_7 L^8 V_{2+1}}{g_s}. \quad (2.14)$$

Two Wess-Zumino terms emerge from various gauge fields and their field strengths. The first Wess-Zumino term is

$$S_{WZ}^{(1)} \sim \int C_4^{(AdS_5)} \wedge F \wedge F \quad (2.15)$$

$$= -\mathcal{N}_7\zeta_7 \int_{r_0}^{\infty} dr\, f_1 f_2 r^4 h\dot{z}. \quad (2.16)$$

We generalize a sign of Ramond-Ramond couplings of the probed branes by introducing ζ_7, where $|\zeta_7| = 1$. It depends on the orientation of the branes, and both branes and anti-branes are considered. Branes and anti-branes have the opposite sign-coefficient for WZ term. These ζ's appear only in the coefficients of the C_p Wess-Zumino terms to indicate they source opposite RR-fields. This topic will be discussed at greater length in the later chapter about $D7/\bar{D}7$-branes pair.

Since the F_5 for the D3-branes background is self-dual, there are two kinds of C_4 on AdS_5 and S^5 in (2.5), Therefore, the emergent second Wess-

Zumino term for F_5 on S^5 is

$$S^{(2)}_{WZ} = \frac{N_7 T_7 (2\pi\alpha')^2}{2} \zeta_7 \int F_5^{(S^5)} \wedge A \wedge F^{(B)} \tag{2.17}$$

$$= 2\mathcal{N}_7 \zeta_7 B \int_{r_0}^{\infty} dr \, \frac{\partial c(\psi)}{\partial \psi} \dot{\psi} A_0(r) \tag{2.18}$$

$$= -2\mathcal{N}_7 \zeta_7 B \int_{r_0}^{\infty} dr \, c(\psi) \dot{A}_0(r) + 2\mathcal{N}_7 \zeta_7 B c(\psi) A_0(r)|_{r_0}^{\infty} \tag{2.19}$$

The full action is

$$S_{D7} = \int_{r_0}^{\infty} dr \, L_7 + 2\mathcal{N}_7 \zeta_7 B c(\psi) A_0(r)|_{r_0}^{\infty} \tag{2.20}$$

where

$$\frac{L_7}{\mathcal{N}_7} = -\sqrt{V(\psi, r)} \sqrt{1 + r^2 h \dot{\psi} + r^4 h \dot{z}^2 - \dot{A}_0^2} - r^4 h \zeta_7 f_1 f_2 \dot{z} - 2\zeta_7 c(\psi) B \, \dot{A}. \tag{2.21}$$

Chapter 3

The Effective Action

3.1 Legendre Transformation and Routhians

Since both $z(r)$ and $A_0(r)$ are cyclic in the Lagrangian (2.21), their conjugate momenta are constant. Especially for the conjugate charge density of the zero component gauge field, we need to be careful to carry out the physical dual charge density in the field theory side. We define it as follows.

$$D = \frac{1}{\mathcal{N}_7}\frac{\delta S}{\delta A_0(\infty)} \tag{3.1}$$

From the action including the boundary term, (2.20), we obtain

$$D = Q_7 + 2\zeta_7 B c_\infty \tag{3.2}$$

where

$$Q_7 \equiv \frac{1}{\mathcal{N}_7}\frac{\delta L_7}{\delta \dot{A}_0} \tag{3.3}$$

$$= \dot{A}_0\sqrt{\frac{V(r,\psi)}{1 + r^2 h\dot{\psi} + r^4 h\dot{z}^2 - \dot{A}_0^2}} - 2\zeta_7 B c(\psi). \tag{3.4}$$

We perform a Legendre transformation for A_0 to make the first Routhian.

$$R_7^{(1)} = -L_7 + \mathcal{N}_7 Q_7 \dot{A}_0 \tag{3.5}$$

$$= -\mathcal{N}_7\sqrt{\Delta_7}\sqrt{V(r,\psi) + \left(Q_7 + 2\zeta_7 c(\psi)B\right)^2} - \mathcal{N}_7 r^4 h\zeta_7 f_1 f_2 \dot{z} \tag{3.6}$$

where $\Delta_7 \equiv 1 + r^2 h\dot{\psi} + r^4 h\dot{z}^2$.

The conjugate momentum of $z(r)$ is defined by

$$P_z \equiv \frac{1}{\mathcal{N}_7}\frac{\delta R_7^{(1)}}{\delta z} \tag{3.7}$$

$$= -\sqrt{V(\psi,r)}\frac{r^4 h\dot{z}}{\sqrt{1+r^4 h\dot{z}^2}} - r^4 h\zeta_7 f_1 f_2 \tag{3.8}$$

Then the second Routhian is

$$R_7^{(2)} = -R_7^{(1)} + \mathcal{N}_7 P_z \dot{z} \tag{3.9}$$

$$= -\mathcal{N}_7\sqrt{1+r^2\dot{\psi}}\sqrt{V(r,\psi)+\left(Q_7+2\zeta_7 c(\psi)B\right)^2 - \frac{(P_z+\zeta_7 f_1 f_2 r^4 h)^2}{r^4 h}} \tag{3.10}$$

P_z vanishes with the black hole embedding, and it has non-zero values with Minkowski embeddings. This kind of the classification defines the phase transition in the gravitational theory. In the appendix, we introduce more general Legendre transformations.

3.2 Linearized Action and Asymptotes

D3/D7-branes configuration is unstable without flux. To clarify this instability, we will expand the second full Routhian to quadratic order in small asymptotic fluctuations of ψ. We will consider only constant $\psi(r)$ solutions to simplify the problem. Since P_z is also constant, we have one dimensional problem now.

To find specific constant solutions for ψ, let us solve equation of motion as a 1-dimensional problem. Legendre transformation is helpful to simplify the equation of motion. The equation of motion for the full Routhian is following. From now on, we will omit subscript $_7$ for the most of field quantities.

$$\frac{1}{\mathcal{N}_7}\frac{\partial R^{(2)}}{\partial\dot{\psi}} = -\frac{r^2 h\dot{\psi}}{\sqrt{1+r^2\dot{\psi}}}\sqrt{V(r,\psi)+\left(Q_7+2\zeta_7 c(\psi)B\right)^2 - \frac{(P_z+\zeta_7 f_1 f_2 r^4 h)^2}{r^4 h}} = 0 \tag{3.11}$$

Therefore,

$$\frac{1}{\mathcal{N}_7}\frac{\partial R^{(2)}}{\partial\psi} = 0 \tag{3.12}$$

and it gives

$$\frac{\partial}{\partial\psi}\Big[V(r,\psi)+\big(Q_7+2\zeta_7 c(\psi)B\big)^2\Big]=0 \tag{3.13}$$

Because the first term of (3.13), $V(r,\psi)$, is dependent on r, and the second term of that, $\big(Q_7+2\zeta_7 c(\psi)B\big)^2$, is independent of r, we can split (3.13) into two independent equations.

$$\frac{\partial V(r,\psi)}{\partial\psi}=8(r^4+B^2)\sin 2\psi\bigg(f_2^2\sin^2\psi-f_1^2\cos^2\psi+\sin^2 2\psi\cos 2\psi\bigg)=0 \tag{3.14}$$

$$\frac{\partial\big(Q_7+2\zeta_7 c(\psi)B\big)^2}{\partial\psi}=2\zeta_7 B\frac{\partial c(\psi)}{\partial\psi}\big(Q_7+2\zeta_7 c(\psi)B\big) \tag{3.15}$$

$$=0=4B\zeta_7(1-\cos 4\psi)\big(Q_7+2\zeta_7 c(\psi)B\big), \tag{3.16}$$

where $c(\psi)\equiv\psi-\frac{1}{4}\sin 4\psi+c_0$.

The equation, (3.14) depends only on ψ with fixed f_1, f_2, so it gives the constant ψ as we assumed. For the second one, (3.16), $\cos 4\psi=1$ or $Q_7+2\zeta_7 c(\psi)B$ with the constant ψ determined by (3.13). The equation (3.14) serves two constant ψ solutions. $\psi=0,\ \pi/2$ satisfy $\sin 2\psi$=0. However, either S^2 of two S^2 vanishes with these two constant solutions, so D7-branes have zero size.

Let us set the constant $\psi=\bar{\psi}$ determined by $f_2^2\sin^2\psi-f_1^2\cos^2\psi+\sin^2 2\psi\cos 2\psi=0$. Now we are ready to expand the second full Routhian to quadratic order in small asymptotic fluctuations of ψ around $\bar{\psi}$.

$$\psi=\bar{\psi}+\phi \tag{3.17}$$

where $|\phi| \ll 1$, and the full Routhian expands to quadratic order as

$$\frac{R^{(2)}}{-\mathcal{N}_7} = \sqrt{1+r^2\dot{\psi}}\sqrt{V(r,\psi) + \left(Q_7 + 2\zeta_7 c(\psi)B\right)^2 - \frac{(P_z + \zeta_7 f_1 f_2 r^4 h)^2}{r^4 h}}$$

$$\equiv \sqrt{1+r^2\dot{\psi}}\; W(r,\psi) \tag{3.18}$$

$$\sim \left(1 + \frac{1}{2}r^2 h\dot{\phi}^2\right)\cdot\left(W(r,\bar{\psi}) + \frac{\partial W}{\partial\psi}|_{\bar{\psi}}\phi + \frac{1}{2}\frac{\partial^2 W}{\partial\psi^2}|_{\bar{\psi}}\phi^2\right) + \mathcal{O}(\phi^3) \tag{3.19}$$

$$\sim \frac{1}{2}\bar{W}(r)r^2 h\dot{\phi}^2 + \frac{\partial\bar{W}}{\partial\psi}\phi + \frac{1}{2}\frac{\partial^2\bar{W}}{\partial\psi^2}\phi^2 \tag{3.20}$$

where $W(r,\psi)|_{\bar{\psi}} \equiv \bar{W}(r)$. This quadratic approximate Routhian is simply Lagrangian of the massive scalar field, ψ.

For large r,

$$\bar{W}(r) = w_1 r^2 + \frac{w_2}{r^2} + \mathcal{O}(\frac{1}{r^6}) \tag{3.21}$$

where

$$w_1 \equiv \sqrt{(f_1^2 + 4\sin^4\bar{\psi})(f_2^2 + 4\cos^4\bar{\psi}) - \zeta_7^2 f_1^2 f_2^2} \tag{3.22}$$

$$= \sqrt{4f_2^2\sin^4\bar{\psi} + 4f_1^2\cos^4\bar{\psi} + 16\sin^4\bar{\psi}\cos^4\bar{\psi}} \tag{3.23}$$

and

$$w_2 = \frac{B^2(f_1^2 + 4\sin^4\bar{\psi})(f_2^2 + 4\cos^4\bar{\psi}) - 2P_z\zeta_7 f_1 f_2 + \left(Q_7 + 2\zeta_7 c(\bar{\psi})B\right)^2 + r_h^4 f_1^2 f_2^2}{2\sqrt{(f_1^2 + 4\sin^4\bar{\psi})(f_2^2 + 4\cos^4\bar{\psi}) - f_1^2 f_2^2}} \tag{3.24}$$

The leading term, $w_1(\bar{\psi})$ is independent of B, ζ_7 and Q. For large r, let us assume $\phi \sim r^{\Delta}(\Delta < 0)$ asymptotically, and a leading term of the equation of motion with respect to ϕ is independent of ϕ, and dependent on w_1,

$$\frac{\partial w_1}{\partial\bar{\psi}}r^2 + \mathcal{O}(r^{2+\Delta}) = 0 \tag{3.25}$$

$$= \frac{8\cos\bar{\psi}\sin\bar{\psi}\Big(f_2^2\sin^2\bar{\psi} - f_1^2\cos^2\bar{\psi} + 4\cos^2\bar{\psi}\sin^2\bar{\psi}(\cos^2\bar{\psi} - \sin^2\bar{\psi})\Big)}{\sqrt{4f_2^2\sin^4\bar{\psi} + 4f_1^2\cos^4\bar{\psi} + 16\sin^4\bar{\psi}\cos^4\bar{\psi}}} = 0 \tag{3.26}$$

It yields

$$f_2^2\sin^2\bar{\psi} - f_1^2\cos^2\bar{\psi} + 4\cos^2\bar{\psi}\sin^2\bar{\psi}(\cos^2\bar{\psi} - \sin^2\bar{\psi}) = 0 \tag{3.27}$$

or

$$\sin 2\bar{\psi} = 0. \tag{3.28}$$

The latter equation yields constant solutions, $\bar{\psi} = 0,\ \pi/2$ that either S^2 of two S^2 vanishes. They are not in our interest. The former equation is also satisfied by (3.14). The leading order does not have any new information.

The next order will depend on Δ, and we will confine our field quantities to stabilize the asymptotic scalar field with this order.

$$w_1 \frac{d}{dr}\big(r^4 \dot{\phi}\big) = r^2 \frac{\partial^2 w_1}{\partial \bar{\psi}^2}\phi, \tag{3.29}$$

in other expression,

$$\Delta(\Delta+3) = \frac{w_1''(\bar{\psi})}{w_1(\bar{\psi})} = \frac{1}{2w_1^2}\frac{\partial^2}{\partial \bar{\psi}^2}(w_1^2) \tag{3.30}$$

in the order of $r^{2+\Delta}$. $\frac{\partial w_1}{\partial \bar{\psi}} = 0$ by the leading order computation, and it yields

$$\Delta(\Delta+3) = \sin^2 2\bar{\psi}\Big(\frac{f_1^2 + f_2^2 - 4\sin^2 2\bar{\psi} + 4\cos^4\bar{\psi} + 4\sin^4\bar{\psi}}{4f_2^2\sin^4\bar{\psi} + 4f_1^2\cos^4\bar{\psi} + 16\sin^4\bar{\psi}\cos^4\bar{\psi}}\Big) \tag{3.31}$$

It is in agreement with [9]. We obtain $f_1^2 = f_2^2$ and the non-trivial asymptotic constant solution $\bar{\psi} = \pi/4$ by using the equation (3.14). $\Delta_\pm$ are obtained from the equation of motion..

$$\Delta_\pm = -\frac{3}{2} \pm \frac{1}{2}\sqrt{9 + 16\frac{f_1^2 + 16\sin^6\bar{\psi} - 12\sin^4\bar{\psi}}{f_1^2 + 4\sin^6\bar{\psi}}}. \tag{3.32}$$

Stability condition requires Δ to be real. In other words, To stable the asymptotic solution, we have

$$|f_1| = |f_2| \leq \sqrt{\frac{23}{50}} \sim 0.678233 \tag{3.33}$$

The magnitudes of the two fluxes are the same. Then two S^2 in D7-branes are balanced each other, and D7-branes should wrap the equatorial $S^2 \times S^2$.

It agrees to $\bar{\psi} = \pi/4$. If the magnitude of the fluxes are smaller than $\sqrt{\frac{23}{50}}$, the D7-branes are unstable because they have a tachyonic mode from the asymptotic fluctuations along the coordinate ψ [9]. This equatorial wrapping of D7-branes is the possible maximal wrapping on $S^2 \times S^2$. If f_i are too big, then Δ_+ will be positive, so this growing solutions are also excluded.

Chapter 4

$D7/\bar{D}7$ branes Model with Constant ψ

4.1 Geometrical Chiral Symmetry and its Breaking

Like Sakai-Sugimoto, we will consider joined D7- and anti D7-branes. However, we do not compactify the 4th coordinate differently from Sakai-Sugimoto model. This corresponds to the decompactified limit. Then, the D-branes model exhibits chiral symmetry breaking more clearly. The supergravity background of it serves a stringy NJL model. The separation of the boundary is dual to effective coupling of 4 fermions interaction. [15] [16] Despite we are surveying a joined branes model, we focus on right hand branch, where z is positive on a z-r plane, so have half of the whole solutions symmetrically.

From now on, we set ψ is constant in the rest of the paper for simplicity. In $D7/\bar{D}7$-branes model, constant $\psi = \pi/4$ as we discussed in the previous chapter. Let us recall the conservative momentum with respect to z coordinate. r_0 is the minimum limit of r, where $D7/\bar{D}7$ branes meet. The momentum depends on values at r_0 is

$$\frac{\partial L}{\partial \dot{z}} = P_z = -\sqrt{V(\psi, r)}\frac{r^4 h\dot{z}}{\sqrt{1 + r^4 h\dot{z}^2}} - r^4 h\zeta_7 f_1 f_2 \tag{4.1}$$

$$= -(r_0^4 - r_h^4)\Big(sgn(\dot{z}_0)\sqrt{\frac{V(\psi_0, r_0)}{r_0^4 - r_h^4}} + \zeta_7 f_1 f_2\Big), \tag{4.2}$$

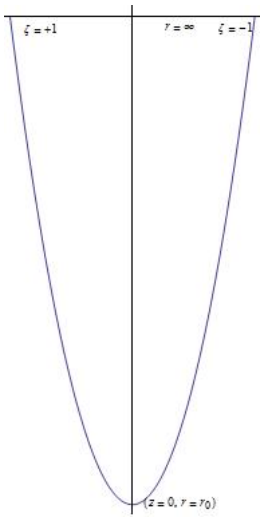

Figure 4.1: **Cartoon of a Skinny joined embedding** We will treat right hand branch, i.e positive z side usually. ζ indicates the orientation of the Ramond fields. In this figure, right hand branch has $\zeta = -1$, and left one has $+1$.

where

$$f_1 = f_2 \tag{4.3}$$

$$z(r_0) = 0^{\text{III}} \tag{4.4}$$

$$\psi(r_0) = \psi_0 \tag{4.5}$$

$$\frac{dz}{dr}(r_0) = \pm\infty^{\text{IV}} \tag{4.6}$$

Solve the equation to get $\dot{z}$, and plug into the full Lagrangian including

WZ terms.

$$\dot{z}^2 = \frac{(P_z + r^4 h\zeta_7 f_1 f_2)^2}{r^4 h\Big(V r^4 h - (P_z + r^4 h\zeta_7 f_1 f_2)^2\Big)} \tag{4.7}$$

$$\dot{z}^{\mathrm{V}} = -(P_z + r^4 h\zeta_7 f_1 f_2)\sqrt{\frac{1}{r^4 h\Big(V r^4 h - (P_z + r^4 h\zeta_7 f_1 f_2)^2\Big)}} \tag{4.8}$$

$$r^4 h\dot{z}^2 = \frac{(P_z + r^4 h\zeta_7 f_1 f_2)^2}{V r^4 h - (P_z + r^4 h\zeta_7 f_1 f_2)^2} \tag{4.9}$$

$$1 + r^4 h\dot{z}^2 = \frac{V r^4 h}{V r^4 h - (P_z + r^4 h\zeta_7 f_1 f_2)^2} \tag{4.10}$$

If the branes pairs do not join, they finally reach the horizon and P_z should vanish because $r_h = r_0$ gives constant momentum $P_z(r_0) = 0$ in (4.2). We call this "black hole embedding" or "straight branes"[VI]. The joined solution exhibits a geometrical chiral symmetry breaking in terms of string theory introduced by Sakai-Sugimoto. By introducing branes/anti-branes pair, it appears that the massless scalar field as Nambu-Goldstone bosons associated with a spontaneous breaking of the $U(N_f)_L \times U(N_f)_R$ chiral symmetry as a gauge symmetry of the branes pairs. In near horizon, finally they meet and smoothly make one branes branch, and only one $U(N_f)_V$ gauge symmetry is left. It is interpreted as spontaneously chiral symmetry breaking. Then straight solution does not meet before the horizon and touched the horizon separately is interpreted as the unbroken chiral symmetry. Therefore, we should carry out these two configurations have different physical phase. To check which configuration is favoured, we should compare the actions(or free energies) of "two" cases, the joined and unjoined ones.

Let us fix $r_h = 1$. It does not affect on physics because r is redundancy does not have physical degree of freedom. Then, now the subtraction between the free energies of both branes configurations will determine which one is favoured in terms of r_0.

[VI] It is not an authentic straight line.

The on-shell action for the joined solution is

$$\frac{S}{N_7} = \int_{r_0}^{\infty} dr - \sqrt{\frac{V^2 r^4 h}{V r^4 h - (P_z + r^4 h \zeta_7 f_1 f_2)^2}} - \zeta_7 f_1 f_2 \sqrt{\frac{(P_z + r^4 h \zeta_7 f_1 f_2)^2 r^4 h}{V r^4 h - (P_z + r^4 h \zeta_7 f_1 f_2)^2}} \tag{4.11}$$

$$= \int_{r_0}^{\infty} dr \big[- V + (P_z + r^4 h \zeta_7 f_1 f_2) \zeta_7 f_1 f_2 \big] \sqrt{\frac{r^4 h}{V r^4 h - (P_z + r^4 h \zeta_7 f_1 f_2)^2}} \tag{4.12}$$

$$= \int_{r_0}^{\infty} dr \big[- V + P_z \zeta_7 F + r^4 h F^2 \big] \sqrt{\frac{r^4 h}{V r^4 h - (P_z + r^4 h \zeta_7 F)^2}} \tag{4.13}$$

where $F = f_1 f_2 = f_1^2 = f_2^2$.

For the straight solution, P_z should vanish because D7-branes reach to the horizon, and $r_h = r_0$ gives $P_z(r_0) = 0$, therefore the action is simply

$$\frac{S_{straight}}{N_7} = \int_{r_h}^{\infty} dr \Big(- V + r^4 h \zeta_7^2 f_1^2 f_2^2 \Big) \sqrt{\frac{r^4 h}{V r^4 h - (r^4 h \zeta_7 f_1 f_2)^2}} \tag{4.14}$$

Then the sign of $\Delta S \equiv S_{straight} - S_{joined}$ is what we should understand for the symmetry breaking phenomena. Before investigating it, however, we should figure out all possible configurations for the joined solutions.

4.2 Skinny, Fat and Fish Solutions

4.2.1 Skinny and fat physical solutions

Let us recall the conservative momentum P_z,(4.2) and $\dot{z}$,(4.8). The sign of $\dot{z}$ at $r = r_0$(equivalently at $z = 0$) geometrically depends on a direction of the branch we choose. If we choose the right one, the sign of $\dot{z}_0$ is positive, otherwise, the opposite. That is, $\dot{z}$ at r_0 is $\pm\infty$ according to whether we observe the right branch($z > 0$) or the other($z < 0$). By (4.8), the sign of $\dot{z}$ is the same as the one of

$$\alpha(r) \equiv -(P_z + r^4 h \zeta_7 f_1 f_2) = -P_z - r^4 h \zeta_7 F. \tag{4.15}$$

As we said briefly in the previous chapter, ζ_7 relates to the sign of Ramond-Ramond couplings for the branes and $|\zeta_7| = 1$. Branes and anti-branes have the opposite sign-coefficient for WZ term.We emphasize that the right branch has the opposite charge of the left branch.

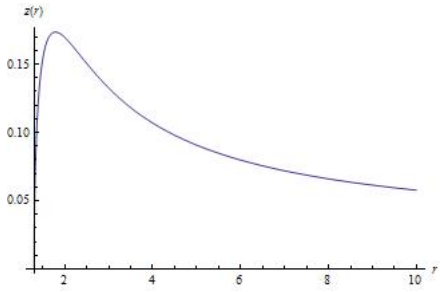

Figure 4.2: Plot of $z(r)$ vs r in the right branch of D7-branes. $f^2 = 0.46$, $\zeta_7 = 1$ and $B = 0$.

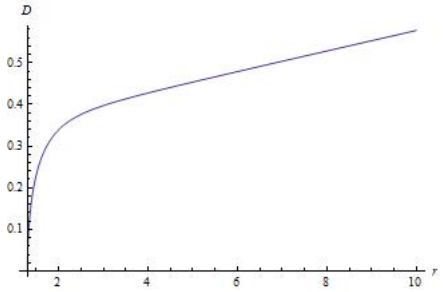

Figure 4.3: Plot of $D \equiv r \times z(r)$. $f^2 = 0.46$, $\zeta_7 = 1$ and $B = 0$.

Since $F = f_1^2 = f_2^2$ is positive, the sign $\dot{z}$ at $r = \infty$ is the same as $-\zeta_7$. Definitely,the sign of $\dot{z}_0$ does not affect the sign of $\dot{z}(\infty)$. The defined function, $\alpha(r)$ is a monotonic, so the sign of $\alpha(r)$ or the sign of $\dot{z}$ can be changed once at most from $r = r_0$ to $r = \infty$. We classify the joined solutions according to whether it changes the sign or not. If changed, "Fat solution", otherwise "Skinny solution". These defining are visually appropriate for the plot $z(r)$ vs r.(See the figure 4.2 to better understand.) Be careful that it does not mean the physical separation between branes/anti-branes also forms like the figure 4.2. We should calculate the metric $ds^2 \sim r^2 dz^2$ on the plane in order to compute the distance. It is still slim-looking from the figure 4.3.

	left branch	right branch
	$z(r) < 0\ , \dot{z}_0 < 0$	$z(r) > 0,\ \dot{z}_0 > 0$
	$P_z > 0$	$P_z < 0$
$\zeta_7 = +1$	$\dot{z}(\infty) < 0 \rightarrow$ "SKINNY!"	$\dot{z}(\infty) < 0 \rightarrow$ "FAT!"
$\zeta_7 = -1$	$\dot{z}(\infty) > 0 \rightarrow$ "FAT!"	$\dot{z}(\infty) > 0 \rightarrow$ "SKINNY!"

Table 4.1: Classification for Skinny/Fat solution of D7-branes joined solutions.

We investigate the momentum on each branch. From the equation (4.2),

$$\begin{aligned} P_z &= P_z\ (\ z = 0, r = r_0) \\ &= -(r_0^4 - r_h^4) F \Big[sign(\dot{z}_0) \sqrt{(1 + \frac{1}{F})^2 \Big(\frac{r_0^4 + B^2}{r_0^4 - r_h^4} \Big)} + \zeta_7 \Big]. \quad (4.16) \end{aligned}$$

The inner term of the square root of the equation (4.16) is definitely larger than 1 if F is non-zero and $|\zeta_7| = 1$. Therefore, P_z is dependent on the sign of $\dot{z}_0$ regardless of ζ_7. That is, the sign of P_z is the opposite of that of $\dot{z}_0$. We summarize all we discussed at the table 4.1.

4.2.2 Fish unphysical solutions

If you are a sophisticated reader, you would have realized that the table 4.1 doesn't cover all possible solutions. The branes can have negative $\dot{z}(\infty)$ on the infinite boundary of the right branch for the fat solution, and $\dot{z}(r)$ becomes positive intermediately on the way to approach the minimum r, r_0, and finally meet the left branch at $r = r_0$ and $z = 0$.

These solutions do not violate the rule we set in the previous section. However, it is unphysical since negative $\dot{z}(\infty)$ does not make sense in the model. $D7/\bar{D}7$ branes pairs join before they reach $r = r_0$. These unphysical solutions will conceptually collapse to small skinny solutions and bubbles. Because we start the numerical test from the point ($r = r_0$,$z = 0$), these fish solutions appear with $z(\infty) = \mp\frac{L}{2}$ on the right(left) branch. We have

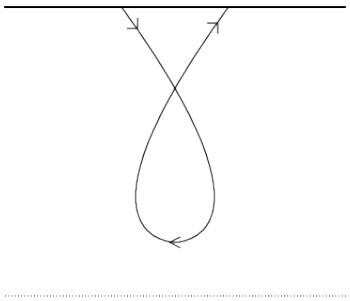

Figure 4.4: Cartoon of a fish solution with negative L.

set the $z(r_0) = 0$, so $\Delta z \equiv z(\infty) - z(r_0) = z(\infty)$ for the right branch.

$$z(\infty) = \int_{r_0}^{\infty} dr\, \dot{z}(r) \tag{4.17}$$

$$= \int_{r_0}^{\infty} dr\, -(P_z + r^4 h \zeta_7 f_1 f_2) \sqrt{\frac{1}{r^4 h (V r^4 h - (P_z + r^4 h \zeta_7 f_1 f_2)^2)}} \tag{4.18}$$

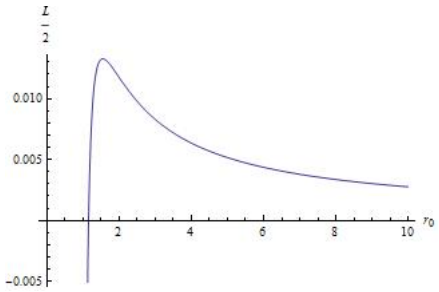

Figure 4.5: Plot of $\frac{L}{2}$ vs r_0 for a skinny solution for $r_h = 1$, $B = 0$ and $F = 0.5$. It approaches zero asymptotically. It makes sense because $r_0 = \infty$ means these branes pair joins near the boundary L does not need to have a size.

When the branes have positive $\dot{z}(\infty)$ on the infinite boundary of the right branch as well, the sign of $\dot{z}$ flips over as well as branes and anti-branes join at $r = r_0$. Figures 4.4 and 4.5 shows this configuration, so called "Fish solution". For $r_h = 1$ and $F = 0.5$, when $r_0 < 1.15518$, $L/2$ is negative (Figure 4.5). It does not happen for the skinny solutions at all. The left

limit for the skinny solutions is always positive, on the other hand it is always negative for the $\zeta_7 = +1$ along the right branch, and the negative line correspond to unphysical fish solution which is not our concerns.

4.3 Magnetic Effect on the $D7/\bar{D}7$-branes Model

4.3.1 Inverse magnetic catalysis in the skinny solutions

Now without loss of generality, we will consider only right branch in table 1. Besides, in this subsection will we focus on skinny solutions, where $\zeta_7 = -1$. Let us go back to the free energy or the action for the straight solution(4.14) and joined solution.(4.13)

$$\frac{S_{joined}}{N_7} = \int_{r_0}^{\infty} dr \left[-(1+F)^2(B^2+r^4) - F\left(F(r^4 - r_h^4) + \left(F - \frac{(1+F)\sqrt{B^2+r_0^4}}{\sqrt{-1+r_0^4}} \right)(r_0^4 - r_h^4) \right) \right] \times \sqrt{\frac{r^4 - r_h^4}{(1+F)^2(B^2+r^4)(r^4-r_h^4) - \left(F(r^4 - r_h^4) + \left(F - \frac{(1+F)\sqrt{B^2+r_0^4}}{\sqrt{-1+r_0^4}} \right)(r_0^4 - r_h^4) \right)^2}} \tag{4.19}$$

$$\frac{S_{straight}}{N_7} = \int_{r_h}^{\infty} dr \; - \sqrt{B^2(1+F)^2 + (1+2F)r^4 + F^2 r_h^4} \tag{4.20}$$

where $F = f^2$.

It is easy to realize both straight embedding and joining embedding have the same ordered(r cube) diverges by using the expanding series at large r. Thus, we can subtract each diverging term and obtain the convergent value. This technique is so called "Regrouping". Because r_h is smaller than r_0, we can integrate the action for the straight solution from r_h to r_0, and can integrate the difference between both actions from r_0 to ∞. Both former and latter can be finite, not divergent. The former integral is analytically

computed.

$$-\int_{r_h}^{r_0} dr\,\sqrt{B^2(1+F)^2+(1+2F)r^4+F^2{r_h}^4} \tag{4.21}$$

$$=\sqrt{r_h^4F^2+B^2(1+F)^2}\Bigg(r_h\times{}_2F_1\left[-\frac{1}{2},\frac{1}{4},\frac{5}{4},-\frac{r_h^4(1+2F)}{r_h^4F^2+B^2(1+F)^2}\right]$$

$$-\,r_0\times{}_2F_1\left[-\frac{1}{2},\frac{1}{4},\frac{5}{4},-\frac{(1+2F)r_0^4}{r_h^4F^2+B^2(1+F)^2}\right]\Bigg), \tag{4.22}$$

where ${}_2F_1\,[a,b,c,d]$ is a hypergeometric function.

The latter, the difference between the free energies of two embeddings, is numerically convergent.

To treat the the infinitely large range for integration, we transform

$$r\to\tilde{r}=\frac{r}{r_0} \tag{4.23}$$

$$\tilde{r}\to y^{-\frac{1}{4}}. \tag{4.24}$$

Then

$$\int_{r_0}^{\infty} dr = r_0\int_1^{\infty} d\tilde{r} = \frac{1}{4}r_0\int_0^1 dy\,y^{-\frac{5}{4}}. \tag{4.25}$$

As we can see in (4.20), we cannot rescale r_h totally from our coordinate transformation.

If ΔS is negative, the joined solution dominates, otherwise, the straight one dominates. We are able to evaluate it numerically(Figure 4.6). We consider $f^2\geq 0.46$ for the stability of the model. When the horizon approaches the joined place, the pair of the probed branes favours a separation, i.e. symmetry restoration.

Of our interest now is the effect from varying fields, the external magnetic field and the fluxes. The asymptotic boundary conditions of the embeddings, $L=2\Delta z(\infty)$ of the joined solutions are the physical quantities altered by field theoretical point of view. The changing field quantities change r_0.

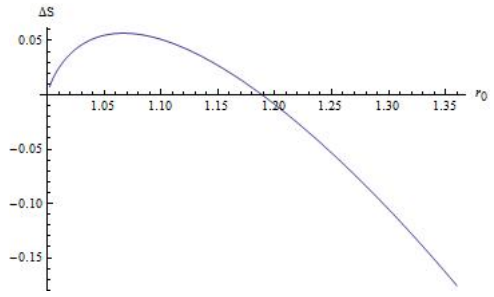

Figure 4.6: Plot of ΔS vs r_0 for a skinny solution.$r_h = 1$, $F = 0.5$ and $B = 0$.

We therefore plot of ΔS vs L to see the clearer effect from altered field quantities.(Figure 4.7)

For $B = 0$, $F = 0.5$ and $r_h = 1$, figure 4.7 shows that when $L > L_c \equiv 0.595265$, the chiral symmetry is broken. $L > 0.640033$ is not in our interests because it does not encourage any joined solution. If $L >$maximum of L, it is unphysical for joined solutions. In other words, $\Delta S = S_{straight}$ for $B = 0$ is positively divergent for $L > 0.640033$ that we will ignore. It indicates we would have the straight solution in $L > 0.640033$, and it makes sense it is already bigger than $L_c = 0.595265$.

Let us see the figure 4.8 that L_c for $B = 10$ is smaller than L_c without the magnetic field. L_c for $B = 10$ is 0.529752. For $L_c(B = 10) < L = 0.55 < L_c(B = 0)$, the chiral symmetry has been restored by the external magnetic field, $B = 10$. $S = S_{straight}$ is positively so divergent for $L > 0.590403$ for $B = 10$. It is lower than the value for $B = 0$.

These exotic phenomena are corroborated by the figure 4.9. L_c is monotonic decreasing with respect to B(at least until 100 order). This result is consistent with the result of [12]. The plot lines in the figure 4.9. can be interpreted as the line between two phases, chiral symmetry phase and broken chiral symmetry phase. Let us assume we have the system with asymptotic boundary L=0.5. For smaller B, it belongs to the area below the plot line in the figure 4.9, where ΔS is negative. In other words, the

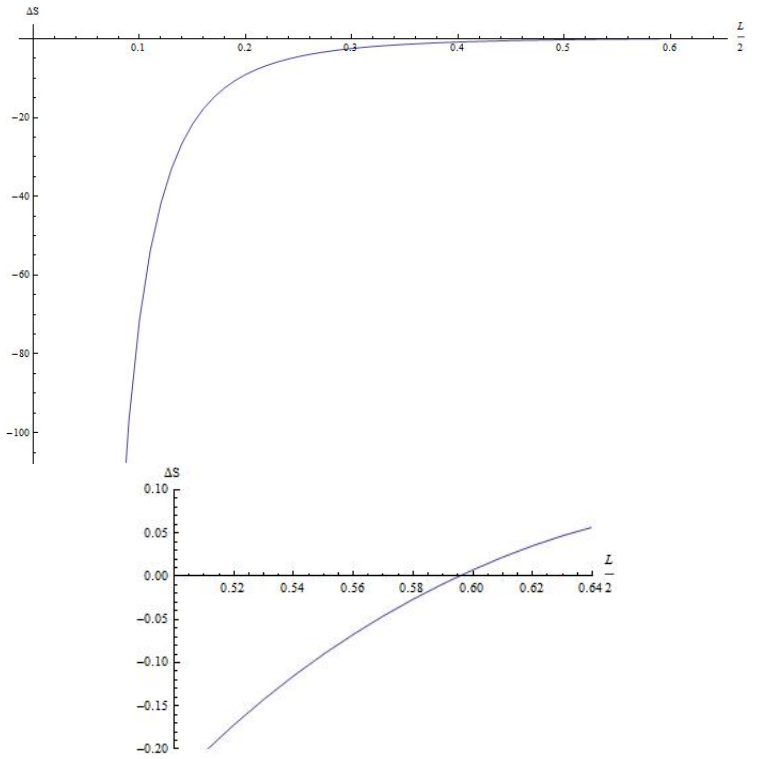

Figure 4.7: Plot of ΔS vs $L/2$ for a skinny solution for $r_h = 1$, $F = 0.5$ and $B = 0$. Second plot is enlarged for the critical part.

joined embeddings are favoured as well as chiral symmetry is broken spontaneously. As the magnetic field increases, L goes over the plot line of L_c, then it favours the straight embeddings and it has chiral symmetry phase. This is the unexpected *inverse magnetic catalysis* in the skinny solutions of the D7-branes pairs.

The same numerical results can be seen from the another plots, the figure 4.10. It shows two plot lines. Let us see the blue(thin) one at first. The external magnetic field B=0 is fixed and the internal fluxes are changeable. We are not interested in $f^2 < 0.46$ as well as $f^2 > 1$. Now as increasing fluxes with a fixed magnetic field, the system favours broken symmetry phase. If we introduce an external magnetic field($B = 10$ in the figure 4.10 for the

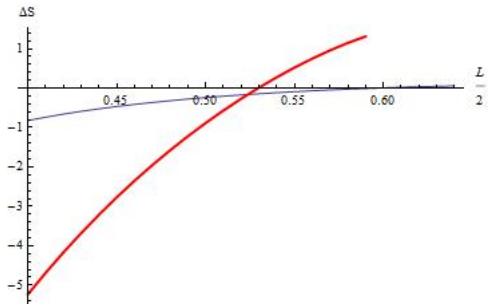

Figure 4.8: Plot of ΔS vs $L/2$ for a skinny solution with two magnetic fields, B=0(blue) and B=10(red and thick). ($r_h = 1$, $F = 0.5$) L_c(Blue)= 0.595265 and L_c(Red)= 0.529752.

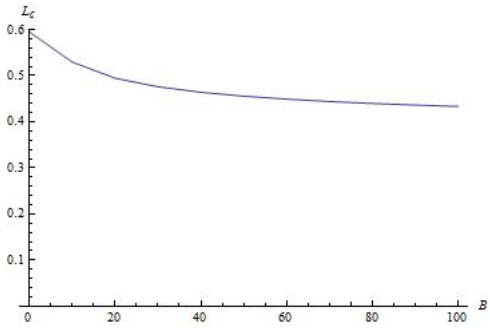

Figure 4.9: Phase diagram with B. Plot of L_c vs B for a skinny solution for $r_h = 1$ and $F = 0.5$.

red plot line), the area for the broken symmetry phase is lowered down. If we have the asymptotic boundary $L = 0.55$ at $f^2 = 0.5$, for B=0 it belongs to broken symmetry phase, but for B=10 the chiral symmetry is restored.

4.3.2 Magnetic catalysis in the fat solutions

We will take $\zeta_7 = +1$ with the right branch for the fat solutions. The procedure to obtain the numerical results is almost the same as we did in the previous subsection for the skinny case. However, the numerical result is critically different(Figure 4.11). It is consistent with the *magnetic catalysis*

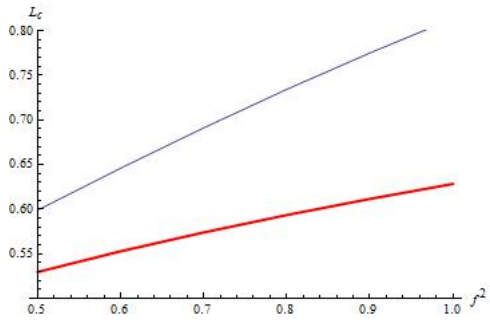

Figure 4.10: Phase diagram with fluxes. Plot of L_c vs $F = f^2$ for a skinny solution for $r_h = 1$. $B = 0$(blue and thin) and $B = 10$(red and thick).

in the chiral field theory.

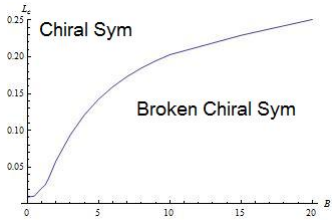

Figure 4.11: Phase diagram with B. Plot of L_c vs B for a fat solution for $r_h = 1$ and $F = 0.5$.

It is so interesting that the magnetic field works reversely for two embedding solutions. Magnetic field might force the branes to be straighten. The magnitude of $\dot{z}$ is in inverse proportion to $|B|$ roughly. In other words, $|\dot{z}|_H < |\dot{z}|_{H=0}$ for each value of r(See the equation (4.8)) regardless of the value of ζ_7, which endows the opposite to the result of the Sakai-Sugimoto model in the presence of the magnetic field researched by [13]. The magnetic field makes the profile $D7/\bar{D}7$-branes less bend, so they meet farther to the boundary. In limit of $B \to \infty$, the configuration of the D3/D7-branes goes to D3/D5-branes which are BPS objects do not have any forces between them. Therefore, we conclude this realization of the magnetic catalysis would work only with relatively small magnetic field. In the figures 4.11 and 4.12, we

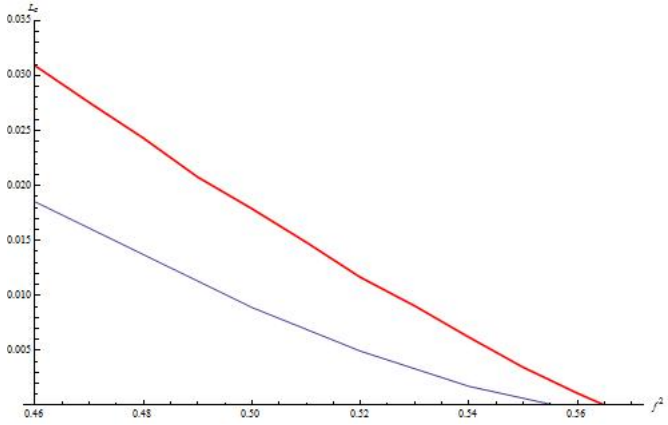

Figure 4.12: Phase diagram with fluxes. Plot of L_c vs $F = f^2$ for a fat solution for $r_h = 1$, $B = 0$(blue) and $B = 1$(red, thick).

verify this conjecture that the effect of the magnetic field is definitely bigger when B is relatively small. What I really mean is that f^2 and B have different order, $f^2 \sim \mathcal{O}(1)$ and $B \sim \mathcal{O}(10)$, to see the definite phenomena in the figures 4.11 and 4.12.

On the other hand, the flux plays a big role here differently from skinny case where the flux does not change much the systems. In the figure 4.12, the plot also shows the opposite numerical result of the skinny solution. Therefore, we have seen both flux and magnetic field work reversely for the fat solution comparing with skinny solutions.

For the skinny solutions, ΔS becomes negative as $r_0 < 2$ regardless of B, F. That is the critical r_0 where ΔS change the sign is quite small. For the fat solutions, however, the critical r_0 becomes bigger very fast(See the figure 4.13 by increasing flux f^2, and this makes L_c approaches zero too close to obtain the more exact numerical result.

To understand these exotic phenomena with fat embedding, we should fully understand how we have the physical fat solutions not collapsed to fish unphysical ones. Let us remind the biggest difference between two solutions

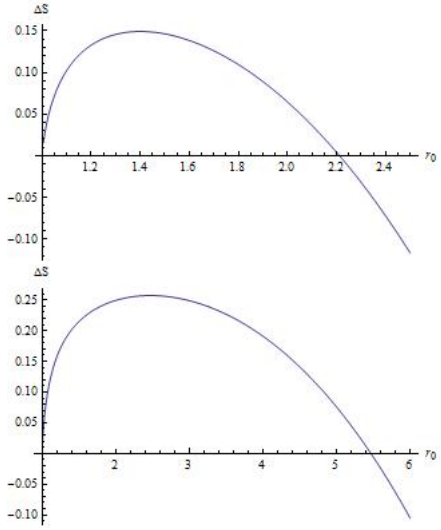

Figure 4.13: Plot of ΔS vs r_0 for a fat solution. $r_h = 1$, $B = 0$ and $F = 0.46$(top) and $F = 0.55$(bottom).

types(skinny or fat/fish) have the opposite signed Ramond-Ramond coefficient, which we have seen at the figure 4.2. We don't have any unphysical solution from skinny case($\zeta_7 = -1$). It favours fish unphysical one for almost r_0. When we increase the flux more, i.e. $f^2 > 0.557243$(numerically obtained), it cannot have any physical fat solution. For $f^2 = 0.6$, the values of L are all negative except for the origin where r_0 is infinite.

It is easier to understand why the *magnetic catalysis* works for the fat/fish solutions by comparing the figures 4.14, 4.15 and 4.16. We turn on the magnetic fields in the systems we introduced in the figure **??** do not have the physical solutions at all. The figure 4.15 makes an affirmation we definitely have the physical solutions. For instance, at $r_0 = 2.5$ at the plots of the figures 4.15 and 4.17, they have positive $L/2$ and negative ΔS favour the physical fat joined solution.

The red(thick) line in the figure 4.12 clarify above numerical results. It corresponds to the fat solutions with an external magnetic field, $B = 1$. As

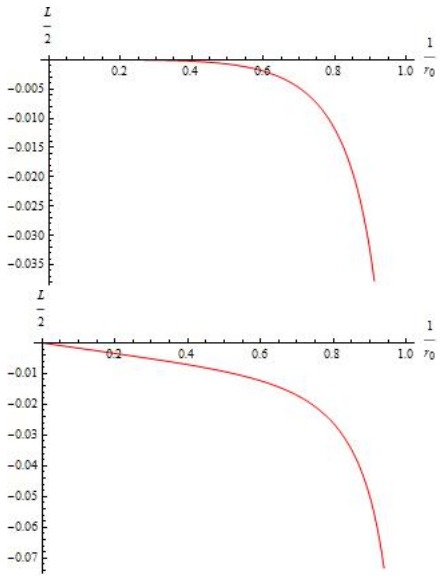

Figure 4.14: Plots of $\frac{L}{2}$ vs r_0 for fat solutions for $r_h = 1$, $B = 0$, $F = 0.5573$(top) and $F = 0.6$(bottom). All L/2 are negative, so we do not have any embedded solution in these plots.

we discussed before, to stabilize the asymptotic solutions with constant ψ, we have $f_1^2 = f_2^2 = 0.46$ regardless of the magnetic fields. Thus, red line also start from $F = f^2 \geq 0.46$. However, the configuration with $B = 1$ has physical solutions with bigger fluxes than the configuration without magnetic field. In more detail as $f^2 = 0.56$, we have the positive L_c in the red(thick) line(for $B = 1$) contrary to no line in the blue thin line(for $B = 0$) in the figure 4.12.

It is very noticeable that every line ends finitely with some specific fluxes in the figure 4.18. When fluxes are bigger than critical values for the fixed magnetic fields, there is no physical fat solution definitely. The plot lines in the figure **??** as well as all plots of L_c vs B or f^2 can be interpreted as the line between two phases, chiral symmetry phase and broken chiral symmetry phase. For non-zero magnetic fields, as we have seen at the figure 4.15, L become negative as r_0 is rather big. Thus, if we find L_c with the

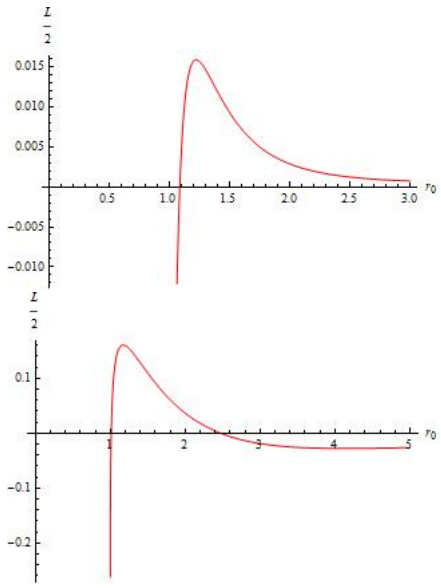

Figure 4.15: Plots of $\frac{L}{2}$ vs r_0 for fat solutions for $r_h = 1$, $F = 0.5573$, $B = 1$(top) and $F = 1$, $B = 10$(bottom).

same way above, we could have negative L_c. Since those embeddings are not constructible, we have cut the negative part in the figures 4.12 and 4.18.

In sum, fat solutions are disfavoured by bigger fluxes, but the external magnetic field helps the physical fat solutions restored with those fluxes. Thus, we regard this as effectively *emergent magnetic catalysis* in the fat solutions.

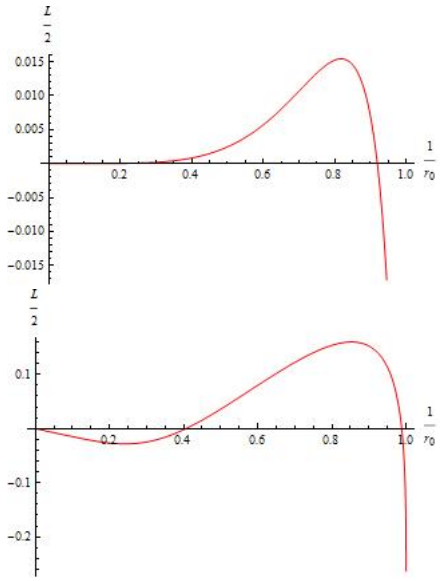

Figure 4.16: The same system with ones in the figure 4.15, i.e. plots of $\frac{L}{2}$ vs r_0 for fat solutions for $r_h = 1$, $F = 0.5573$, $B = 1$(top) and $F = 1$, $B = 10$(bottom). but used the $1/r_0$ axis to see all range of r_0.

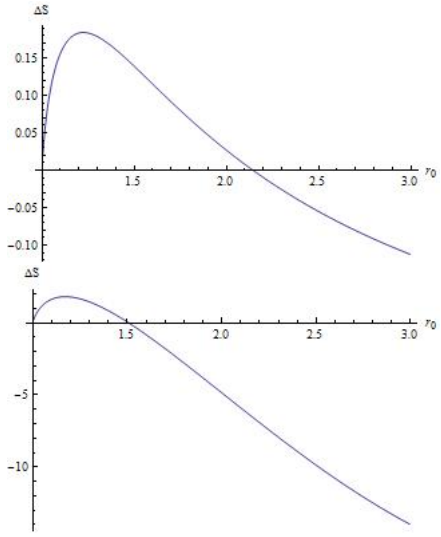

Figure 4.17: Plot of ΔS vs r_0 for fat solutions. $r_h = 1$, $F = 0.557253$, $B = 1$(top) and $F = 1$, $B = 10$(bottom).

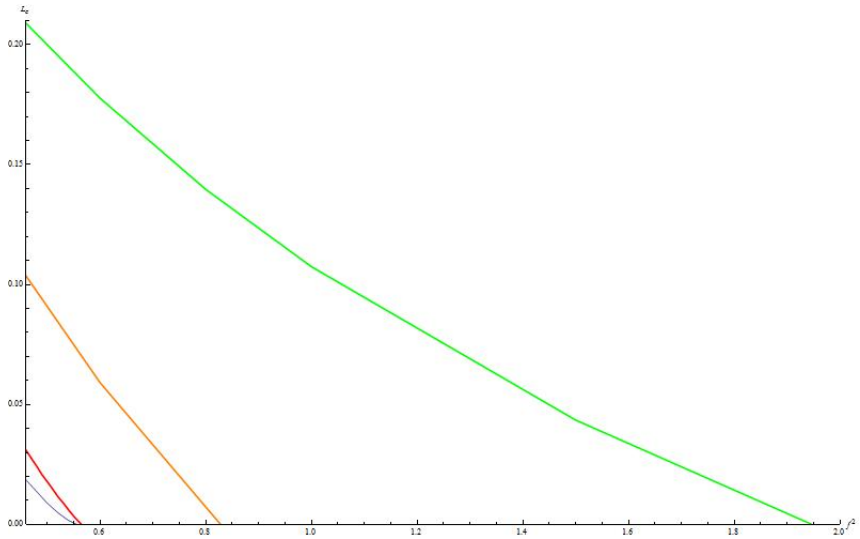

Figure 4.18: Phase diagram with a flux. Plot of L_c vs $F = f^2$ for a fat solution for $r_h = 1$, $B = 0$(blue), $B = 1$(red, thick), $B = 3$(Orange) and $B = 10$(Green).

Chapter 5

Construction of D3/D5-branes model

D3/D5-branes system has been researched in various ways. It is worth considering D5-brane as a probe on the D3-branes supergravity background in the similar way to the D3/D7-branes model. Thus we used the same thermal D3-branes background except for Chern-Simons terms since we have only one flux on S^2.

$$L^{-2}ds^2 = r^2\big(-h(r)dt^2 + dx^2 + dy^2 + dz^2\big) + \frac{dr^2}{h(r)r^2} + d\Omega_5^2 \tag{5.1}$$

where

$$h(r) = 1 - \frac{r_h^4}{r^4} \tag{5.2}$$

$$L^4 = 4\pi g_s N_3 \alpha'^2 \tag{5.3}$$

$$d\Omega_5^2 = d\psi^2 + \sin^2\psi d\Omega_2^2 + \cos^2\psi d\tilde{\Omega}_2^2 \tag{5.4}$$

$$F_5 = dC_4 = \frac{4L^4}{g_s}(r^3 dt \wedge dx \wedge dy \wedge dz \wedge dr) \tag{5.5}$$

$$\frac{g_s}{L^4}C_4 = r^4 h(r) dt \wedge dx \wedge dy \wedge dz \tag{5.6}$$

$$\begin{array}{rc} & 0\,1\,2\,3\,4\,5\,6\,7\,8\,9 \\ D3 & \bullet\bullet\bullet\bullet - - - - - - \\ D5 & \bullet\bullet\bullet - \bullet\bullet\bullet - - - \end{array} \tag{5.7}$$

We employ the same probe *ansatz* with the D3/D7-branes model, $z = z(r)$ and $\psi = \psi(r)$, and suppose constant ψ. D5-branes extend along t, x, y and wraps one S^2.

The external magnetic field and the electric field with fluxes on S^2 is

$$F = F_{rt}(r)dr \wedge dt + F_{xy}(r)dx \wedge dy + F_{\theta\phi}(r)d\theta \wedge d\phi \tag{5.8}$$

$$= \frac{L^2}{2\pi\alpha'}\Big(\dot{A}_0(r)dr \wedge dt + B\, dx \wedge dy + \frac{f}{2}d\Omega_2\Big). \tag{5.9}$$

The induced metric on the D5-branes are described by

$$L^{-2}ds^2 = r^2\big(-h(r)dt^2 + dx^2 + dy^2\big) + \frac{1 + r^2h\dot{\psi}^2 + r^4h\dot{z}^2}{h(r)r^2}dr^2 + \sin^2\psi d\Omega_2^2 \tag{5.10}$$

and the full Lagrangian is

$$\frac{L_5}{\mathcal{N}_5} = -\sqrt{V(\psi, r)}\sqrt{1 + r^2h\dot{\psi} + r^4h\dot{z}^2 - \dot{A}_0^2} - r^4h\zeta_5 f\dot{z} \tag{5.11}$$

where

$$V(\psi, r) = (r^4 + B(r)^2)(f^2 + 4\sin^4\psi) \tag{5.12}$$

$$\mathcal{N}_5 = \frac{2\pi N_5 T_5 L^6 V_{2+1}}{g_s}. \tag{5.13}$$

$$Q_5 \equiv \frac{1}{\mathcal{N}_5}\frac{\delta L_5}{\delta \dot{A}_0} = \dot{A}_0\sqrt{\frac{V(r,\psi)}{1 + r^2h\dot{\psi} + r^4h\dot{z}^2 - \dot{A}_0^2}} \tag{5.14}$$

5.1 The Effective Action

The first Routhian we obtained from the Legendre transformation with respect to A_0 is,

$$R_5^{(1)} = -L_5 + \mathcal{N}_5\, Q_5\, \dot{A}_0 \tag{5.15}$$

$$= -\mathcal{N}_5\sqrt{1 + r^2h\dot{\psi} + r^4h\dot{z}^2}\sqrt{V(r,\psi) + Q_5^2} - \mathcal{N}_5 r^4h\zeta_5 f\dot{z} \tag{5.16}$$

The conjugate momentum of the $z(r)$ for the D5 branes is defined by

$$P_z \equiv \frac{1}{\mathcal{N}_5}\frac{\delta R_5^{(1)}}{\delta z} \tag{5.17}$$

$$= -\sqrt{V(\psi,r)}\frac{r^4 h\dot{z}}{\sqrt{1+r^4 h\dot{z}^2}} - r^4 h\zeta_5 f \tag{5.18}$$

Then the second Routhian we obtain from the Legendre transformation with respect to z is

$$R_5^{(2)} = -R_5^{(1)} + \mathcal{N}_5 P_z \dot{z} \tag{5.19}$$

$$= -\mathcal{N}_5\sqrt{1+r^2\dot{\psi}}\sqrt{V(r,\psi)+Q_5^2 - \frac{(P_z+\zeta_5 f r^4 h)^2}{r^4 h}} \tag{5.20}$$

5.1.1 Linearized action and asymptotes

D3/D7-branes configuration is unstable without flux, but D3/D5-branes configuration is stable regardless of the presence of flux.[VII] My point in the D3/D7-branes model was that the existence of flux on two 2-spheres is essential to stabilize the systems, but we do not have such necessity on the D3/D5-branes model. Nevertheless, we will introduce an external magnetic field and fluxes repeatedly to better understand the phenomena of the joined solutions with various an external magnetic field and fluxes.

To clarify it, we expand the second full Routhian to quadratic order in small asymptotic fluctuations of ψ again. By assumption, $\psi(r)$ =constant to simplify the problem. Similarly to the case of the D7-branes, we will omit subscript $_5$ for the most of field quantities.

$$\frac{1}{\mathcal{N}_5}\frac{\partial R^{(2)}}{\partial\dot{\psi}} = -\frac{r^2 h\dot{\psi}}{\sqrt{1+r^2\dot{\psi}}}\sqrt{V(r,\psi)+Q_5^2 - \frac{(P_z+\zeta_5 f r^4 h)^2}{r^4 h}} = 0 \tag{5.21}$$

[VII] Speaking rigorously, for the fat solutions it is incorrect, because it is unstable with bigger flux than some specific flux as we have seen through $D7/\bar{D}7$-branes model.

Therefore,

$$\frac{1}{\mathcal{N}_5}\frac{\partial R^{(2)}}{\partial \psi} = 0 \tag{5.22}$$

by the Lagrange equation, and it yields

$$\begin{aligned}
\frac{\partial}{\partial \psi}\left[V(r,\psi) + Q_5^2\right] &= -16(r^4 + B^2)\cos^3\psi \sin\psi && (5.23)\\
&= -8(r^4 + B^2)\cos^2\psi \sin 2\psi && (5.24)\\
&= -4(r^4 + B^2)(1 + \cos 2\psi)\sin 2\psi && (5.25)\\
&= 0
\end{aligned}$$

Thus, the constant ψ solutions are specifically $\psi = 0,\ \pi/2$. The former one $\psi = 0$ means the two sphere wrapped by D5-branes vanishes. Therefore the only possible constant solution for this model is $\psi = \pi/2$ which D5-branes wrap the maximal S^2. It is in agreement with the D3/D5-model described in [8]. Now we are ready to expand the second full Routhian to quadratic order in small asymptotic fluctuations of ψ around the $\bar{\psi} = \pi/2$.

$$\psi = \bar{\psi} + \phi \tag{5.26}$$

where $|\phi| \ll 1$, and the full Routhian expands to quadratic order as

$$\begin{aligned}
-\frac{R^{(2)}}{\mathcal{N}_5} &= \sqrt{1 + r^2\dot{\psi}}\sqrt{V(r,\psi) + Q_5^2 - \frac{(P_z + \zeta_7 f r^4 h)^2}{r^4 h}}\\
&\equiv \sqrt{1 + r^2\dot{\psi}}\ W(r,\psi) && (5.27)\\
&\sim \left(1 + \frac{1}{2}r^2 h\dot{\phi}^2\right)\cdot\left(W(r,\bar{\psi}) + \frac{\partial W}{\partial \psi}|_{\bar{\psi}}\phi + \frac{1}{2}\frac{\partial^2 W}{\partial \psi^2}|_{\bar{\psi}}\phi^2\right) + \mathcal{O}(\phi^3) && (5.28)\\
&\sim \frac{1}{2}\bar{W}(r) r^2 h\dot{\phi}^2 + \frac{\partial \bar{W}}{\partial \psi}\phi + \frac{1}{2}\frac{\partial^2 \bar{W}}{\partial \psi^2}\phi^2. && (5.29)
\end{aligned}$$

For large r,

$$\bar{W}(r) = w_1 r^2 + \frac{w_2}{r^2} + \mathcal{O}(\frac{1}{r^6}) \tag{5.30}$$

where

$$\begin{aligned}
w_1 &\equiv \sqrt{f^2 + 4\sin^4\bar{\psi} - \zeta_5^2 f^2} && (5.31)\\
&= \sqrt{4\sin^4\bar{\psi}} = 2\sin^2\bar{\psi} && (5.32)
\end{aligned}$$

The leading term, $w_1(\bar{\psi})$ is independent of B, ζ_5, Q_5 and even f.

The next order will depend on Δ, and we will confine our field quantities to stabilize the asymptotic scalar field with this order.

$$w_1 \frac{d}{dr}\left(r^4 \dot{\phi}\right) = r^2 \frac{\partial^2 w_1}{\partial \bar{\psi}^2}\phi, \tag{5.33}$$

in other expression,

$$\Delta(\Delta+3) = \frac{w_1''(\bar{\psi})}{w_1(\bar{\psi})} = -2 \tag{5.34}$$

in the order of $r^{2+\Delta}$. Thus, $\Delta = -2, -1$. It agrees with [8] that $m^2 = -\frac{2}{L^2_{AdS_4}}$, and it satisfies the BF bound in the asymptotic AdS_4 geometry as an induced metric of the D5-branes. Therefore, we do not have any restriction for the magnitude of the flux on S^2 differently from the case for D7-branes.

Chapter 6

$D5/\bar{D}5$-branes model with constant ψ

The momentum with respect to z for the $D5/\bar{D}5$-branes model is also conserved since the coordinate z is still cyclic in the Lagrangian and Routhians.

$$\frac{\partial L_5}{\partial \dot{z}} = P_z = -\sqrt{V(\psi, r)}\frac{r^4 h \dot{z}}{\sqrt{1 + r^4 h \dot{z}^2}} - r^4 h \zeta_5 f \tag{6.1}$$

$$= -(r_0^4 - r_h^4)\Big(sgn(\dot{z}_0)\sqrt{\frac{V(\psi_0, r_0)}{r_0^4 - r_h^4}} + \zeta_5 f\Big) \tag{6.2}$$

Solve the equation to get $\dot{z}$, and plug it into the full Lagrangian including WZ terms.

$$\dot{z}^2 = \frac{(P_z + r^4 h \zeta_5 f)^2}{r^4 h\Big(V r^4 h - (P_z + r^4 h \zeta_5 f)^2\Big)} \tag{6.3}$$

$$\dot{z} = -(P_z + r^4 h \zeta_5 f)\sqrt{\frac{1}{r^4 h\Big(V r^4 h - (P_z + r^4 h \zeta_5 f)^2\Big)}} \tag{6.4}$$

We should compare the action or free energy of the straight solutions and the joined ones in order to see whether the joined solution is stable or not. The on-shell action for the joined solution is

$$\frac{S_{join}}{\mathcal{N}_5} = \int_{r_0}^{\infty} dr - \sqrt{\frac{V^2 r^4 h}{Vr^4h - (P_z + r^4 h\zeta_5 f)^2}} - \zeta_5 f \sqrt{\frac{(P_z + r^4 h\zeta_5 f)^2 r^4 h}{Vr^4h - (P_z + r^4 h\zeta_5 f)^2}} \tag{6.5}$$

$$= \int_{r_0}^{\infty} dr \Big[-V + (P_z + r^4 h\zeta_5 f)\zeta_5 f \Big] \sqrt{\frac{r^4 h}{Vr^4h - (P_z + r^4 h\zeta_5 f)^2}} \tag{6.6}$$

$$= \int_{r_0}^{\infty} dr \Big[-V + P_z\zeta_5 f + r^4 h f^2 \Big] \sqrt{\frac{r^4 h}{Vr^4h - (P_z + r^4 h\zeta_5 f)^2}} \tag{6.7}$$

$F = f^2 = f_1^2 = f_2^2$ was positive for the $D3/D7$-branes model, so we concerned the sign of ζ_7, but now instead, we should concern the sign of the product of ζ_5 and f, i.e. $\zeta_5\, f$. For the straight solution, $P_z = 0$ because D5-branes reach to the horizon, so the action is

$$\frac{S_{straight}}{\mathcal{N}_5} = \int_{r_h}^{\infty} dr \Big(-V + r^4 h f^2 \Big) \sqrt{\frac{r^4 h}{Vr^4h - (r^4 h f)^2}} \tag{6.8}$$

As confirming before, the action for the straight solutions is independent of ζ, the orientation.

By (6.4), the sign of $\dot{z}$ is the same as that of

$$\alpha_5(r) \equiv -(P_z + r^4 h\zeta_5 f) = -P_z - r^4 h\zeta_5 f. \tag{6.9}$$

As we mentioned earlier, the sign $\dot{z}$ at $r = \infty$ is the same as the sign of $-\zeta_5 f$. The classification for all solutions(skinny, fat and fish type) is almost the same as D7-branes case except that $\zeta_5\, f$ is replaced by ζ_7. From the equation (6.2),

$$\begin{aligned} P_z = P_z\,(\, z = 0, r = r_0) \\ = -(r_0^4 - r_h^4)|f| \Big[sign(\dot{z}_0) \sqrt{(1 + \frac{4}{f^2})\Big(\frac{r_0^4 + B^2}{r_0^4 - r_h^4}\Big)} + \zeta_5 \frac{f}{|f|} \Big]. \end{aligned} \tag{6.10}$$

This formula (6.10) also supports that the sign of P_z is not altered in this model considering D5-branes. We obtain the summarized table 6.1.

	left branch	right branch
	$z(r) < 0$, $\dot{z}_0 < 0$	$z(r) > 0,\ \dot{z}_0 > 0$
	$P_z > 0$	$P_z < 0$
$\zeta_5 f = +1$	$\dot{z}(\infty) < 0 \rightarrow$ "SKINNY!"	$\dot{z}(\infty) < 0 \rightarrow$ "FAT!"
$\zeta_5 f = -1$	$\dot{z}(\infty) > 0 \rightarrow$ "FAT!"	$\dot{z}(\infty) > 0 \rightarrow$ "SKINNY!"

Table 6.1: Classification for Skinny/Fat solution for $D5/\bar{D}5$-branes pair.

6.1 Magnetic Effect on the $D5/\bar{D}5$-branes Model

In this section, we will introduce the numerical results for the D5-branes joined solution. The computational results for the $D5/\bar{D}5$-branes model on $\dot{z}$, ΔS, P_z are almost the same as those for $D7/\bar{D}7$-branes model. They are little different each other only at some constants given by different constant solution for ψ, and have different S^2 embedding. In other words, the D7-branes wrap equatorial $S^2 \times S^2$ with $\psi = \pi/4$ and that the D5-branes wrap maximal S^2 with $\psi = \pi/2$. As a result, we expect $D5/\bar{D}5$-branes model might not be much different from the $D7/\bar{D}7$-branes model.

6.1.1 Numerical plots of the fat solutions

In fat solutions, the last statement of the previous section is true. We will introduce only few plots for this model. We can obtain the main ideas from the plot of L_c vs B or f.

All numerical results for the fat solutions yield the same conclusion with the $D7/\bar{D}7$-branes model. The only difference we have found is the slight change of the magnitude of critical f where $L_c = 0$. By the way, for skinny solutions, we will see the different numerical result.

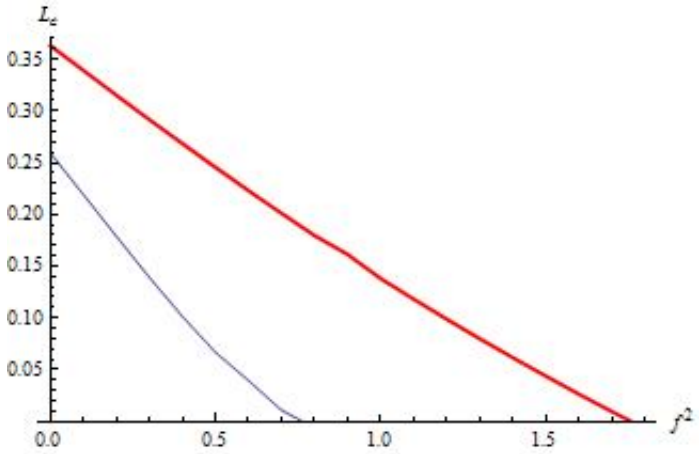

Figure 6.1: Plot of L_c vs B for D5-branes fat joined solutions. $f = 0.5$ We see both magnetic catalysis and inverse one.

6.1.2 Numerical plots of the skinny solutions

Let us see the figure 6.2. Comparing with the figure 4.11, the lines for the various external magnetic fields cross each other. Roughly as f is bigger than 0.6, we can see the same numerical result we have seen in the figure 4.11. L_c is smaller as B is bigger. It shows the inverse magnetic catalysis again. However, when f is smaller than 0.4, L_c is the biggest when B is the biggest $B = 10$. These plots verify the fat joined solutions for the $D5/\bar{D}5$-branes model show the magnetic catalysis phenomenon.

By the way, it is hard to discern which phenomenon is favoured around $f = 0.5$ since we chose only three values for the magnetic fields in the figure 6.2. To better understanding, see the next figure 6.3. In this case, we can see both phenomena in one plot. Magnetic catalysis in the region of smaller magnetic fields, and the inverse magnetic catalysis in that of bigger magnetic fields.

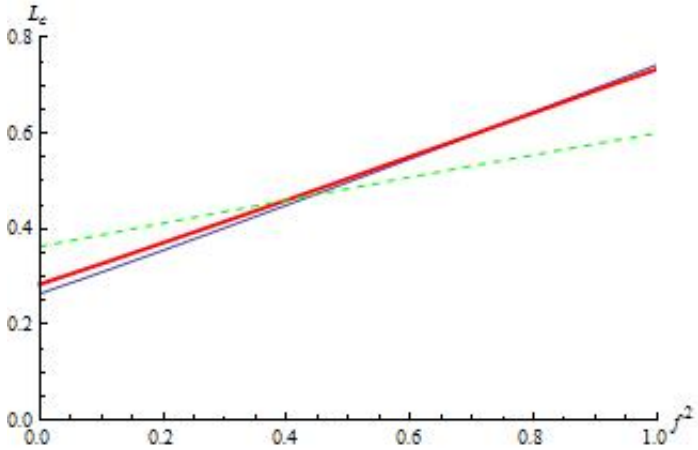

Figure 6.2: Plot of L_c vs f. $B = 0$(Blue and thin). $B = 1$(Red and thick). $B = 10$(green and dashed.

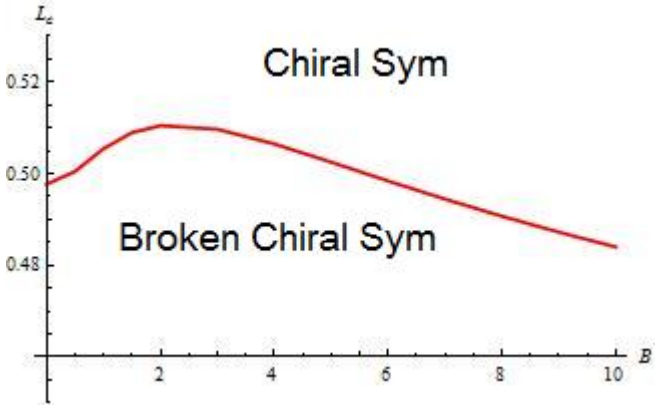

Figure 6.3: Plot of L_c vs B. $f = 0.5$ We see both magnetic catalysis and inverse one.

Chapter 7

Conclusion : Summary, the Domain Wall Configuration and the Perspective

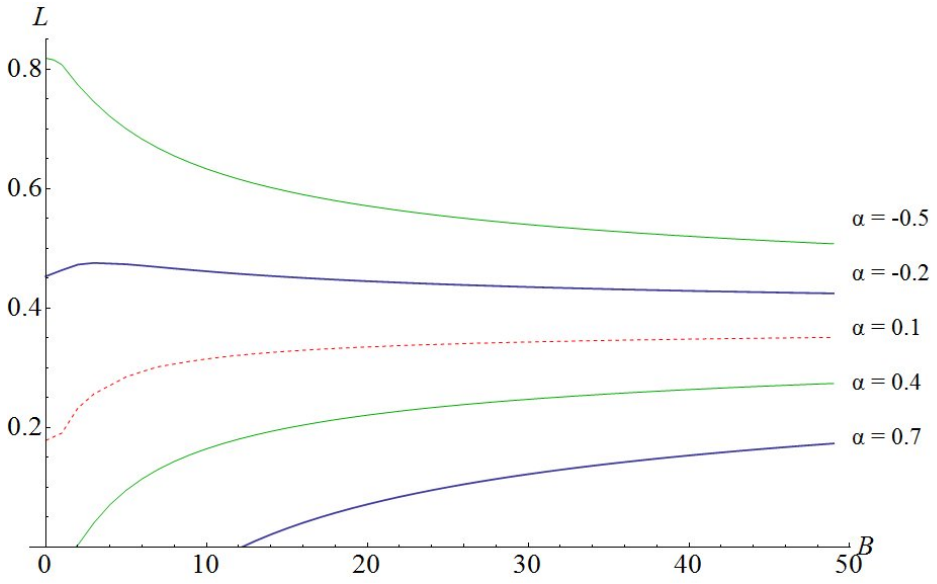

Figure 7.1: Phase diagrams for the defect system. Above any fixed curve, the dominant solution is given by the two disconnected brane worldvolumes, i.e. the symmetric phase. The joined solutions, the broken symmetry phase, dominates below the curve.

Each curve is at fixed α[VIII], above the curve being the flavour symmetric phase where the stacks do not join while below the curve the symmetry is broken to the diagonal subgroup by brane recombination. We can see that for α negative, the stacks always join at small enough L. This is quite intuitive since the background F_5 assists the native attraction of the brane and anti-brane so there is no effect to prevent their joining. On the other hand, we see that for large enough positive α, the stacks do not join at small L unless there is also a strong enough external magnetic field. Intuitively, the force from the background F_5 is strong enough to overcome the brane/anti-brane attraction even at arbitrarily small separation.

We studied D7- and D5-branes models including internal fluxes and an external magnetic fields. Introducing these kinds of internal fluxes on S^2 can be important in the field theory. First of all, they yield magnetic monopoles. It is one of the most simple topological objects we can consider. Now we can regard those probe branes as a charged effective D3-branes. These charged probe branes contribute to the overall Ramond-Ramond flux of the system.

We use flux quantization conditions [8], [9]

$$f = \frac{2\pi\alpha'}{L^2}\frac{n}{N_k} \tag{7.1}$$

on the probe Dk-branes, where n is integer and N_k is the number of the probed branes. For D7-branes, we have two f's and two n's. We used $\mathcal{O}(1)$-fluxes all over this paper. Since α' is so small, the integers as the quantized magnetic charges are very huge by (7.1). It is related to the supergravity limit for the AdS/CFT conjecture, and means we can treat f as a constant parameter in our models.

Let us recall the induced metric for D5-branes probed on thermal D3-

[VIII] α is a parameter to briefly generalize relations of ζ and fluxes. From above investigations did we find these joined model have a common aspect. To better understand the generalization, see [18]

branes background.

$$ds^2_{D5} = \frac{r^2}{L^2}(-h(r)dt^2 + dx^2 + dy^2 + dz^2) + (\frac{L^2}{r^2 h(r)} + \frac{r^2}{L^2}z'(r)^2)dr^2 + L^2 d\Omega_2^2 \tag{7.2}$$

when the radius of horizon is zero, $r_h = 0$, the equation of motion with respect to z yields

$$z'(r) = \frac{L^2 f}{r^2} \tag{7.3}$$

The induced metric corresponds to $AdS_4 \times S^2$ with an AdS radius of curvature $L_{AdS} = L\sqrt{1+f^2}$.

$$ds^2_{D5} = \frac{r^2}{L^2}(-dt^2 + dx^2 + dy^2) + L^2(1+f^2)\frac{dr^2}{r^2} + L^2 d\Omega_2^2 \tag{7.4}$$

With this supersymmetric profile, we obtained $z(r) = -L^2 f/r$. Assume $f > 0$. If we include back reaction, asymptotically with respect to z, the five form flux should be changed $N_c \to N_c + n$. Without the supersymmetric profile, i.e. if we consider thermal D3-branes background at finite temperature, we would see the same result asymptotically in terms of the charges carried by the flux added to Ramond-Ramond charges. It is very interesting and important we can interpret this charge shift as the change of the rank of a gauge group in the dual CFT, $SU(N_c) \to SU(N_c+n)$ in the region indicated by $z(r)$ probing coordinate.(See 7.1) Using the example we introduced above, since the region of $z(r)$ is negative, we have $U(N_c)$ gauge theory as $z > 0$. Thus, if we have the probed multiple charged defects, we have a spatially symmetry breaking pattern in the dual field theory.[8]

Now it is so natural to think the joined solution in terms of the finite-width domain wall of the dual field theory. The 2+1 dimensional world volume of the defect conformal field theory can be interpreted as the domain wall of the 3+1 dimensional conformal field theory. We should be careful we didn't introduce the orientation, ζ in above simple model. Let us consider the skinny joined solution at first, then the charges carried by the flux has the same sign with the Ramond-Ramond charges and we have a contribution

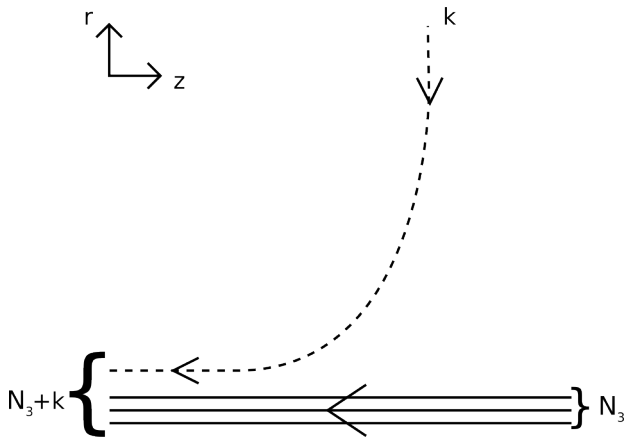

Figure 7.2: A cartoon representation of a probe brane (dashed line) carrying D3-charge k bending to become parallel with the stack of N_3 D3-branes sourcing the AdS geometry, represented by the solid lines at the bottom. The arrows represent brane worldvolume orientation. The dual gauge group is $SU(N_3)$ toward the right while it is enhanced to $SU(N_3 + k)$ to the left.

given by anti-branes, so we have $U(N_c + 2n)$ gauge theory inside the joined solution 2+1 dimensional hypersurface. On the other hand, for the fat joined solution, we have $U(N_c - 2n)$ gauge theory inside the joined solution since the orientation of the probed branes and the sign of the charges carried by the fluxes are the opposite to those of the background D-branes. It will help us to understand the physics of graphene which is described by emergent massless 2+1-dimensional Dirac fermions.

In this paper, we have seen some exotic phase transitions arose in holographic model. It is not clear from the point of view of the field theory what dictates whether the system exhibits *catalysis* or *inverse catalysis*. We will refrain from speculating on the exact mechanism here and leave this question to future work. It can be good methods to investigate more on this model that ones study transport properties on the various joined brane-model or calculate correlation functions on the holographic CFT.

Bibliography

J. Maldacena, Adv. Theor. Math. Phys. 2, 231 (1998) [Int. J. Theor. Phys. 38, 1113 (1998)] ; arXiv:hep-th/971120.

G. W. Semenoff, Phys. Rev. Lett. 53 2449 (1984).

K. Jensen, A. Karch, D. T. Son, and E. G. Thompson(2010); arXiv:hep-th/1002.3159.

A. Karch and E. Katz, "Adding flavor to AdS/CFT," JHEP 0206, 043 (2002) ;arXiv:hep-th/0205236.

E. Witten, Adv. Theor. Math. Phys. 2 (1998), 505; hep-th/9803131.

T. Sakai and S. Sugimoto, Low energy hardron physics in holographic QCD, Prog. Theor. Phys. 113, 843(2005); hep-th/0412141

O. Aharony, J. Sonnenschein and S. Yankielowicz, A holographic model of deconfinement and chiral symmetry restoration; arXiv:hep-th/0604161

R. C. Myers and M. C. Wapler, "Transport Properties of Holographic Defects," JHEP 0812, 115 (2008) ;arXiv:hep-th/0811.0480.

O. Bergman, N. Jokela, G. Lifschytz and M. Lippert, "Quantum Hall Efect in a Holographic Model," ;arXiv:hep-th/1003.4965.

V. P. Gusynin, V. A. Miransky, and I. A. Shovkovy, Phys. Rev. Lett. 73, 3499 (1994); Phys. Rev. D 52, 4718 (1995).

V. P. Gusynin, V. A. Miransky, and I. A. Shovkovy, Phys. Lett. B 349, 477 (1995).

Florian Preis, Anton Rebhan, Andreas Schmitt, Inverse magnetic catalysis in dense holographic matter, JHEP 03 (2011) 033 ; arXiv:hep-th/1012.4785.

C. V. Johnson and A. Kundu, External Fields and Chiral Symmetry Breaking in the Sakai-Sugimoto Model, JHEP 12 (2008) 053 ;arXiv:hep-th/0803.0038.

S.Y. Rey, Quantum Phase Transitions from String Theory, talk at Strings 2007 :http://www.ift.uam.es/strings07/010 marco.htm

S.Y. Rey, Prog. Theor. Phys. Suppl. 177, 128 (2009) ;arXiv:hep-th/0911.5295

E. Antonyan, J. A. Harvey, S. Jensen and D. Kutasov,NJL and QCD from string theory, ; arXive:hep-th/0604017.

E. Antonyan, J. A. Harvey and D. Kutasov,The Gross-Neveu model from string theory, ; arXiv: hep-th/0608149

E. Antonyan, J. A. Harvey and D. Kutasov,Chiral symmetry breaking from intersecting D-branes, ; arXiv:hep-th/0608177

J. L. Davis, M. Gutperle, P. Kraus and I. Sachs, Stringy NJL and Gross-Neveu models at finite density and temperature, JHEP 0710, 049 (2007) ;arXiv:hep-th/0708.0589

J. Polchinski, theory. Vol. 2: Superstring theory and beyond," Cambridge, UK: Univ. Pr. (1998) 531 p.

J. L. Davis, N. Kim, Flavor-symmetry Breaking with Charged Probes, ; arXiv:hep-th/1109.4952

Appendix A

Legendre Transforms

We used the Routhian in the body of the paper to explain the effective Lagrangians. Here we generally introduce how to compute the Legendre transforms for a particular square root Lagrangian which appears frequently in brane embeddings, i.e. from the DBI Lagrangian, and geodesic equations. Such problems come down to an effective one dimensional Lagrangian mechanics problem where the role of time is played by some radial or angular coordinate, which we'll call τ to be definite. The embedding coordinates and other possible worldvolume degrees of freedom (such as gauge fields) we'll denote collectively by $\phi^i(\tau)$.

Our first model Lagrangian is

$$L = -\sqrt{\Upsilon + g_{ij}\dot{\phi}^i\dot{\phi}^j} \tag{A.1}$$

with dots being derivatives w.r.t τ and g_{ij} and Υ functions of the ϕ^i, and even τ explicitly, but not the $\dot{\phi}^i$ for which the transform is being done. That is, Υ could depend on $\dot{x}$ if the Legendre transform will only be for y and z. We assume that g_{ij} is an invertible matrix. Each ϕ has a conjugate momentum given by

$$P_i \equiv \frac{\partial L}{\partial \dot{\phi}^i} = -\frac{g_{ij}\dot{\phi}^j}{\sqrt{\Upsilon + g_{ij}\dot{\phi}^i\dot{\phi}^j}} = \frac{g_{ij}\dot{\phi}^j}{L} \tag{A.2}$$

We can invert (A.2) to get

$$\dot{\phi}^i = Lg^{ij}P_j \tag{A.3}$$

with g^{ij} the matrix inverse of g_{ij}. Substituting this into (A.1) gives

$$L = -\sqrt{\Upsilon + L^2 g^{ij} P_i P_j} \tag{A.4}$$

which we can solve for L to get

$$L = -\sqrt{\frac{\Upsilon}{1 - g^{ij} P_i P_j}} \tag{A.5}$$

We can then easily compute the Hamiltonian

$$\begin{aligned} -H &\equiv L - P_i \dot{\phi}^i \\ &= L\left(1 - g^{ij} P_i P_j\right) \\ &= -\sqrt{\Upsilon}\sqrt{1 - g^{ij} P_i P_j} \end{aligned} \tag{A.6}$$

Similarly, but with a more tedious computation, we can take a Lagrangian with a term which sometimes arises from the Wess-Zumino action,

$$L = -\sqrt{\Upsilon + g_{ij}\dot{\phi}^i \dot{\phi}^j} + \alpha_i \dot{\phi}^i \tag{A.7}$$

where, as in (A.1), we allow Υ, g_{ij} and α_i to depend on ϕ^i but not the derivatives. We get the Hamiltonian

$$\begin{aligned} -H &\equiv L - P_i \dot{\phi}^i \\ &= -\sqrt{\Upsilon}\sqrt{1 - g^{ij}\left(P_i - \alpha_i\right)\left(P_j - \alpha_j\right)} \end{aligned} \tag{A.8}$$

Finally, an even more complicated example

$$L = -\sqrt{\Upsilon + 2\beta_i \dot{\phi}^i + g_{ij}\dot{\phi}^i \dot{\phi}^j} + \alpha_i \dot{\phi}^i + \Gamma \tag{A.9}$$

Again, the undetermined parameters can be functions of the ϕ's but not $\dot{\phi}$'s. This can be reduced to the previous case by defining

$$\begin{aligned} \tilde{\Upsilon} &= \Upsilon - g^{ij}\beta_i \beta_j \\ \dot{\chi}^i &= \dot{\phi}^i + g^{ij}\beta_j \\ \tilde{L} &= L + g^{ij}\alpha_i \beta_j - \Gamma \end{aligned} \tag{A.10}$$

and we get the form (A.7), with

$$\tilde{L} = -\sqrt{\tilde{\Upsilon} + g_{ij}\dot{\chi}^i\dot{\chi}^j} + \alpha_i\dot{\chi}^i \tag{A.11}$$

Then (A.8) tells us that

$$\begin{aligned} -\tilde{H} &\equiv \tilde{L} - \tilde{P}_i\dot{\chi}^i \\ &= -\sqrt{\tilde{\Upsilon}}\sqrt{1 - g^{ij}\left(\tilde{P}_i - \alpha_i\right)\left(\tilde{P}_j - \alpha_j\right)} \end{aligned} \tag{A.12}$$

where

$$\tilde{P}_i = \frac{\partial\tilde{L}}{\partial\dot{\chi}^i} \tag{A.13}$$

Now note that

$$\frac{\partial\tilde{L}}{\partial\dot{\chi}^i} = \frac{\partial L}{\partial\dot{\phi}^i} \tag{A.14}$$

so that $\tilde{P} = P$. Then we have

$$\begin{aligned} -\tilde{H} &\equiv \tilde{L} - \tilde{P}_i\dot{\chi}^i \\ &= L + g^{ij}\alpha_i\beta_j - P_i\left(\dot{\phi}^i + g^{ij}\beta_j\right) - \Gamma \\ &= -H + g^{ij}\left(\alpha_i - P_i\right)\beta_j - \Gamma \end{aligned} \tag{A.15}$$

Then from (A.12) we have

$$\begin{aligned} -H &= -\tilde{H} + g^{ij}\left(P_i - \alpha_i\right)\beta_j \\ &= -\sqrt{\tilde{\Upsilon}}\sqrt{1 - g^{ij}\left(\tilde{P}_i - \alpha_i\right)\left(\tilde{P}_j - \alpha_j\right)} + g^{ij}\left(P_i - \alpha_i\right)\beta_j + \Gamma \\ &= -\sqrt{\Upsilon - g^{ij}\beta_i\beta_j}\sqrt{1 - g^{ij}\left(P_i - \alpha_i\right)\left(P_j - \alpha_j\right)} + g^{ij}\left(P_i - \alpha_i\right)\beta_j + \Gamma \end{aligned} \tag{A.16}$$

Appendix B

$D3/\bar{D}3$-branes Model

B.1 Construction of D3/D3-model and the Full Effective Action

The phenomenon from various fields in above D5-, D7-branes pair model was complicated not to obtain the analytical results. To better understand above branes/anti-branes model, we need to look into $D3/\bar{D}3$-branes model on the thermal D3-branes background, where we don't need to introduce the flux. It is the simplest we can consider with external magnetic field and construction on the plane of $r(z)$ and z.

$$L^{-2}ds^2 = r^2\big(-h(r)dt^2 + dx^2 + dy^2 + dz^2\big) + \frac{dr^2}{h(r)r^2} + d\Omega_5^2 \tag{B.1}$$

where

$$h(r) = 1 - \frac{r_h^4}{r^4} \tag{B.2}$$

$$L^4 = 4\pi g_s N_3 \alpha'^2 \tag{B.3}$$

$$d\Omega_5^2 = d\psi^2 + \sin^2\psi d\Omega_2^2 + \cos^2\psi d\tilde{\Omega}_2^2 \tag{B.4}$$

$$F_5 = dC_4 = \frac{4L^4}{g_s}(r^3 dt \wedge dx \wedge dy \wedge dz \wedge dr) \tag{B.5}$$

$$\frac{g_s}{L^4}C_4 = r^4 h(r) dt \wedge dx \wedge dy \wedge dz \tag{B.6}$$

This model still give the defect 2+1 dimensional conformal field theory,

and the defect constructions are described by the following array:

$$\begin{array}{c} 0\,1\,2\,3\;\;4\;\;5\;\;6\;\;7\;\;8\;\;9 \\ D3\;\bullet\bullet\bullet\bullet\;-\;-\;-\;-\;-\;-\;- \\ D5\;\bullet\bullet\bullet-\;\bullet\;-\;-\;-\;-\;- \end{array} \tag{B.7}$$

We use the probe *ansatz*, $z = z(r)$. D3-probe branes extend along t, x, y and r.

$$F = F_{rt}(r)dr \wedge dt + F_{xy}(r)dx \wedge dy \tag{B.8}$$

$$= \frac{L^2}{2\pi\alpha'}\big(\dot{A}_0(r)dr \wedge dt + B\, dx \wedge dy\big). \tag{B.9}$$

The induced metric on D3-branes are described by

$$L^{-2}ds^2 = r^2\big(-h(r)dt^2 + dx^2 + dy^2\big) + \frac{1 + r^2h\dot{\psi}^2 + r^4h\dot{z}^2}{h(r)r^2}dr^2 \tag{B.10}$$

and the full Lagrangian is

$$\frac{L_3}{\mathcal{N}_f} = -\sqrt{r^4 + B^2}\sqrt{1 + r^2h\dot{\psi} + r^4h\dot{z}^2 - \dot{A}_0^2} - r^4h\zeta_3\dot{z} \tag{B.11}$$

where

$$\mathcal{N}_f = \frac{N_fT_fL^4V_{2+1}}{g_s}.^{\text{IX}} \tag{B.12}$$

$$Q_f \equiv \frac{1}{\mathcal{N}_f}\frac{\delta L_3}{\delta\dot{A}_0} = \dot{A}_0\sqrt{\frac{r^4 + B^2}{1 + r^2h\dot{\psi} + r^4h\dot{z}^2 - \dot{A}_0^2}} \tag{B.13}$$

The first Routhian we obtained from the Legendre transformation w.r.t A_0 is,

$$R_3^{(1)} = -L_3 + \mathcal{N}_f\, Q_3\, \dot{A}_0 \tag{B.14}$$

$$= -\mathcal{N}_f\sqrt{1 + r^2h\dot{\psi} + r^4h\dot{z}^2}\sqrt{r^4 + B^2 + Q_3^2} - \mathcal{N}_fr^4h\zeta_3\dot{z} \tag{B.15}$$

[IX] I will avoid to use $\mathcal{N}_3$, N_3 and T_3 since it is confusing with the number of D3-branes as a thermal sugergravity background.

The conjugate momentum of $z(r)$ for D5-branes is defined by

$$P_z \equiv \frac{1}{\mathcal{N}_f}\frac{\delta R_3^{(1)}}{\delta z} \tag{B.16}$$

$$= -\sqrt{r^4+B^2}\frac{r^4 h\dot{z}}{\sqrt{1+r^4 h\dot{z}^2}} - r^4 h\zeta_3 \tag{B.17}$$

Then the second Routhian is

$$R_3^{(2)} = -R_3^{(1)} + \mathcal{N}_f P_z \dot{z} \tag{B.18}$$

$$= -\mathcal{N}_5\sqrt{1+r^2\dot{\psi}}\sqrt{r^4+B^2+Q_3^2-\frac{(P_z+\zeta_3 h)^2}{r^4 h}} \tag{B.19}$$

B.2 $D3/\bar{D}3$-branes Model

We introduced $D3/\bar{D}3$-branes model here in the appendix, to help understanding D5-, D7-branes model in the body of the paper. The momentum with respect to z for the $D3/\bar{D}3$-branes model is also conserved since z is still cyclic in the Lagrangian and Routhians.

$$\frac{\partial L_3}{\partial \dot{z}} = P_z = -\sqrt{r^4+B^2}\frac{r^4 h\dot{z}}{\sqrt{1+r^4 h\dot{z}^2}} - r^4 h\zeta_3 \tag{B.20}$$

$$= -(r_0^4 - r_h^4)\Big(sgn(\dot{z}_0)\sqrt{\frac{r_0^4+B^2}{r_0^4-r_h^4}} + \zeta_3\Big) \tag{B.21}$$

Solve the equation to get $\dot{z}$, and plug into the full Lagrangian including WZ terms.

$$\dot{z}^2 = \frac{(P_z + r^4 h\zeta_3)^2}{r^4 h\Big(r^4 h(r^4+B^2) - (P_z+r^4 h\zeta_3)^2\Big)} \tag{B.22}$$

$$\dot{z} = -(P_z + r^4 h\zeta_3)\sqrt{\frac{1}{r^4 h\Big(r^4 h(r^4+B^2) - (P_z+r^4 h\zeta_3)^2\Big)}} \tag{B.23}$$

To see the joined solution is stable or not, we should compare the action or free energy of the straight solutions and the joined ones.

The on-shell action for the joined solution is

$$\begin{aligned}
&\frac{S_{join}}{\mathcal{N}_f} = \frac{S_{DBI}}{\mathcal{N}_f} + \frac{S_{WZ}}{\mathcal{N}_f} \\
=&\int_{r_0}^{\infty} dr - \sqrt{\frac{(r^4+B^2)^2 r^4 h}{r^4 h(r^4+B^2)-(P_z+r^4 h\zeta_3)^2}} - \zeta_3 \sqrt{\frac{(P_z+r^4 h\zeta_3)^2 r^4 h}{r^4 h(r^4+B^2)-(P_z+r^4 h\zeta_3)^2}} && \text{(B.24)} \\
=&\int_{r_0}^{\infty} dr \Big[-r^4 - B^2 + (P_z + r^4 h\zeta_3)\zeta_3 \Big] \sqrt{\frac{r^4 h}{r^4 h(r^4+B^2)-(P_z+r^4 h\zeta_3)^2}} && \text{(B.25)} \\
=&\int_{r_0}^{\infty} dr \Big[-r^4 - B^2 + P_z\zeta_3 + r^4 h \Big] \sqrt{\frac{r^4 h}{r^4 h(r^4+B^2)-(P_z+r^4 h\zeta_3)^2}} && \text{(B.26)} \\
=&\int_{r_0}^{\infty} dr \Big[-r_h^4 - B^2 + P_z\zeta_3 \Big] \sqrt{\frac{1}{r^4+B^2-\frac{(P_z+r^4 h\zeta_3)^2}{r^4 h}}} && \text{(B.27)}
\end{aligned}$$

Now what we should concern is the only ζ_3 to classify physical solutions, skinny and fat ones.

For the straight solution, $P_z = 0$ because D3-branes reach to the horizon, therefore the action is following.

$$\begin{aligned}
\frac{S_{straight}}{\mathcal{N}_f} &= \int_{r_h}^{\infty} dr \Big(-r_h^4 - B^2 \Big) \sqrt{\frac{r^4 h}{r^4 h(r^4+B^2)-(r^4 h)^2}} && \text{(B.28)} \\
&= \int_{r_h}^{\infty} dr \Big(-r_h^4 - B^2 \Big) \sqrt{\frac{r^4 h}{r^4 h(r_h^4+B^2)}} && \text{(B.29)} \\
&= \int_{r_h}^{\infty} dr - \sqrt{r_h^4 + B^2} && \text{(B.30)}
\end{aligned}$$

Thus, we can see definitely the free energy for the straight embedding is linearly divergent. The free energy for the joined embedding should be linearly divergent in order to have finite ΔS.

By (B.23), the sign of $\dot{z}$ is the same as that of

$$\alpha_3(r) \equiv -(P_z + r^4 h\zeta_3) = -P_z - r^4 h\zeta_3. \tag{B.31}$$

The sign $\dot{z}$ at $r = \infty$ is the same as the sign of $-\zeta_3$. From the equation (B.21),

$$\begin{aligned}
P_z &= P_z\,(\,z = 0,\, r = r_0) \\
&= -(r_0^4 - r_h^4)\Big[sign(\dot{z}_0) \sqrt{\frac{r_0^4 + B^2}{r_0^4 - r_h^4}} + \zeta_3 \Big]. && \text{(B.32)}
\end{aligned}$$

	left branch	right branch
	$z(r) < 0$, $\dot{z}_0 < 0$	$z(r) > 0,\ \dot{z}_0 > 0$
	$P_z > 0$	$P_z < 0$
$\zeta_3 = +1$	$\dot{z}(\infty) < 0 \rightarrow$ "SKINNY!"	$\dot{z}(\infty) < 0 \rightarrow$ "FAT!"
$\zeta_3 = -1$	$\dot{z}(\infty) > 0 \rightarrow$ "FAT!"	$\dot{z}(\infty) > 0 \rightarrow$ "SKINNY!"

Table B.1: Classification for Skinny/Fat solution for $D3/\bar{D}3$-branes pair.

This formula (B.32) also support that the sign of P_z is not changed in this model considered D3 -branes. Strictly speaking, P_z can be zero as $B = 0$, $r_h = 0$, and the sign of $\dot{z}_0$ and ζ_3 are opposite each other. In this case, P_z can have either sign of positive or negative. We obtain the table summarized.

This model does not look different from the previous two models for D5-, D7-branes pairs. However, unfortunately, ΔS is linear divergent positively regardless of the value of B, $r_0 > r_h = 1$ for both fat and skinny types. It is easy to check because we can calculate the integration as the analytic function. It is divergent at r-infinity. Since ΔS is positive, the straight solutions dominate. However, the straight solution is also unphysical in this model. $\dot{z}(r)$ is also obtained analytically. It is constant, so it yields infinite Δz, L.